5 Cosmic-Ray-Produced Noble Gases in Meteorites

Rainer Wieler

Isotope Geology, ETH-Zürich
Sonneggstrasse 5
CH-8092 Zürich, Switzerland
wieler@2erdw.ethz.ch

INTRODUCTION

Energetic particles of the galactic cosmic radiation (GCR) have a mean penetration depth in rock of about 50 cm, comparable to the typical size of a meteorite. GCR-induced effects therefore provide a means to study the history of meteorites as small objects in space or in the top few meters of their parent body. These effects include cosmic ray tracks, i.e., the radiation damage trails in a crystal lattice produced by heavy ions in the GCR (Fleischer et al. 1975), and thermoluminescence, i.e., the light emitted by a heated sample which had been irradiated by energetic particles (Benoit and Sears 1997). By far most important, however, are "cosmogenic" nuclides, produced by interactions of primary and secondary cosmic ray particles with target atoms.

This chapter concentrates on the cosmogenic noble gas nuclides in meteorites. A separate chapter in this book by Niedermann (2002) discusses cosmogenic noble gases in terrestrial rocks, which are by now a major tool in quantitative geomorphology. Cosmogenic noble gases in lunar samples are briefly presented in the chapter by Wieler (2002) on noble gases in the solar system. Here and in the other chapters mentioned, cosmogenic radionuclides such as ^{10}Be, ^{26}Al, or ^{36}Cl are often also considered, as comprehensive studies usually require combining noble gas and radionuclide analyses. Not further discussed here are cosmic-ray-induced shifts of the abundances of stable isotopes of a few elements besides noble gases. The most important of these are Gd, Sm, and Cd, which have isotopes with extremely high cross sections for the capture of slow (thermal or epithermal) neutrons produced as secondary cosmic ray particles by interactions of the primary GCR protons with target atoms (Eugster et al. 1970; Hidaka et al. 1999; Sands et al. 2001). Because the flux of thermal and epithermal neutrons peaks at greater depths than that of more energetic particles, neutron-induced shifts are mainly produced at relatively high shielding and are thus particularly useful to study the exposure history of large meteorites or a previous exposure stage near the surface of a meteorite parent body (see *Cosmogenic noble gases produced by capture of low-energy neutrons* subsection).

Sometimes, cosmic-ray-induced isotope shifts are also a nuisance, because they may compromise the precise determinations of isotopic compositions of elements of interest. This is often a major problem in the case of "trapped" noble gases (Ott 2002, this volume), but may also require attention when e.g., small excesses or deficits of daughter isotopes of an extinct radionuclide present in the early solar system are to be determined (e.g., Leya et al. 2000c).

In the following, we will first discuss the production systematics of cosmogenic nuclides in meteorites. Next, we will present the distributions of cosmic ray exposure ages of different meteorite classes and discuss what they tell us about meteorite transport from the various parent bodies to Earth. We will also consider so-called "complex" or "pre-exposure" histories, which is when a meteorite also contains cosmogenic nuclides acquired before it became the body with the size and shape it had immediately before it fell to Earth. Some of these meteorites represent material that once was within the top

1529-6466/02/0047-0005$05.00 DOI:10.2138/rmg.2002.47.5

few meters of the surface of their parent body and thus contain information on asteroidal or planetary surface processes. Other meteorites with complex exposure histories may even record an intense irradiation by energetic particles from the early Sun. We will also see how cosmogenic nuclides are used to study the history of the particles that produced them, e.g., possible temporal variations in the fluxes of the cosmic radiation. In the last section, cosmogenic noble gases produced by energetic particles from the Sun (in rather recent times) are briefly mentioned. Earlier reviews on cosmogenic nuclides in extraterrestrial samples include Anders (1962), Reedy et al. (1983), Vogt et al. (1990), Marti and Graf (1992), and chapters 6 and 9 in Tuniz et al. (1998).

THE PRODUCTION OF COSMOGENIC NUCLIDES IN METEORITES

Fundamentals

In this section we discuss how cosmogenic nuclides are produced in solid matter in space and how production rates can be determined for a given sample. The major challenge is that production rates depend on the size of a preatmospheric meteorite (meteoroid) and the position of a given sample within this body, collectively somewhat loosely called the "shielding" of the sample. Since a meteoroid may lose well over 90% of its preatmospheric mass when passing through the Earth's atmosphere, and moreover may disintegrate into many fragments, the shielding is a priori unknown and has to be assumed or deduced by some means.

The shielding dependence of production rates is illustrated in Figure 1, which shows the production rates of ^{21}Ne, P(^{21}Ne), in chondrites and iron meteorites, as well as the

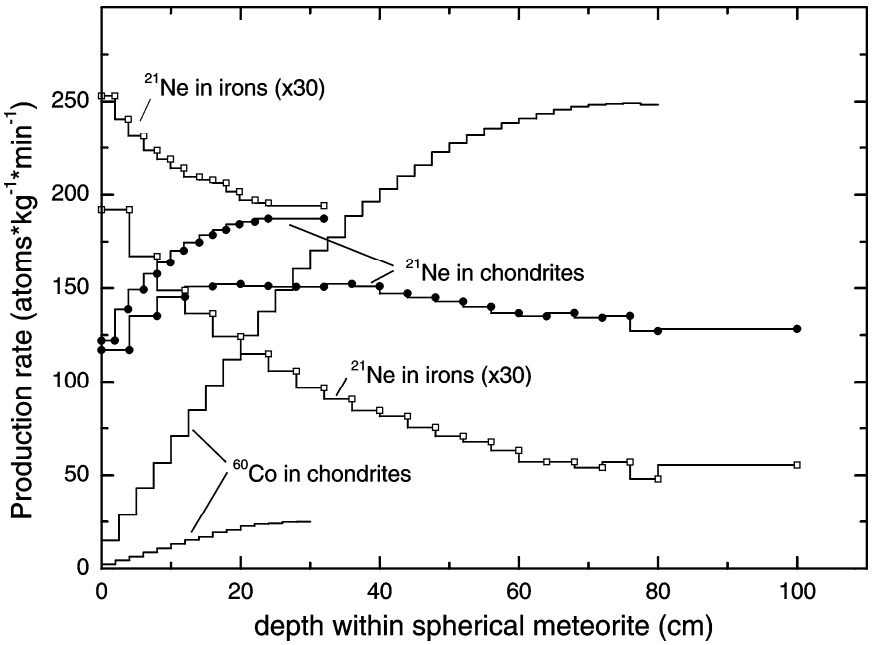

Figure 1. Production rates by galactic cosmic rays of ^{60}Co in chondrites and ^{21}Ne in chondrites and iron meteorites. Two curves are shown for each nuclide-target combination, representing spherical meteorites of two different radii (30 and 80 cm for ^{60}Co, 30 and 100 cm for ^{21}Ne). P(^{21}Ne) in iron meteorites has been multiplied by a factor of 30. The ^{60}Co curves are based on the nuclide production model by Masarik and Reedy (1994), assuming a Co concentration of 690 μμg/g, and the ^{21}Ne curves are calculated with the model by Leya et al. (2000a). The figure illustrates that depth-and size-dependencies of production rates may be highly dissimilar for different nuclides or different nuclide-target combinations.

production rate of the radionuclide ^{60}Co (half-life 5.3 yr) in chondrites. The two curves for each nuclide correspond to spherical meteorites with two different radii (equal to the largest depth shown) and the production rates are calculated by models to be discussed in more detail below (Leya et al. 2000a; Masarik and Reedy 1994). Cosmogenic nuclides in meteorites are produced by protons and alpha-particles of the primary GCR (see also Niedermann 2002) as well as the resulting cascade of secondary protons and neutrons that develops within the meteoroid. The relative contributions from primaries and secondaries can be highly different for various target-nuclide combinations, which is the reason for the widely different shapes of the various curves. The production rate of ^{21}Ne in iron meteorites is highest at the surface and decreases more or less exponentially with depth. This is because ^{21}Ne from iron is a so-called "high-energy product," made preferentially by high energy particles (mostly primary protons), because the mass difference between the target elements (Fe and Ni) and the product ^{21}Ne is large. In contrast, P(^{21}Ne) in chondrites increases from the surface up to ~20- to 40-cm depth, and then decreases less steeply than in iron meteorites. This increase is due to a large contribution by secondary neutrons and protons with lower energies than primary protons, as there is a relatively small mass difference between ^{21}Ne and the main target elements for this nuclide in rocks (Mg, Al, and Si). The much higher absolute production rates in chondrites compared to iron meteorites (whose ordinate values in Figure 1 have been multiplied by a factor of 30) illustrate that production rates also strongly depend on the elemental composition of the target. Generally, production rates are higher when the mass difference between target and product is small, e.g., P(^{21}Ne) from Mg is ~2-3 times higher than P(^{21}Ne) from Si and several ten times higher than P(^{21}Ne) from Fe. Note also that production rates at the surface are higher for smaller bodies (especially smaller iron meteorites) because they see a higher flux of particles from the "opposite" side of the meteoroid.

Whereas the increase of the ^{21}Ne production rate with depth near the surface is modest, and P(^{21}Ne) is somewhat smaller at all depths in the larger body in Figure 1 compared to the smaller one, the variations of P(^{60}Co) with meteoroid size and sample depth are dramatic, e.g., P(^{60}Co) in the center of the R = 80 cm meteoroid is about 10 times higher than in the center of the R = 30 cm body. This is because this nuclide is mostly produced when ^{59}Co captures secondary cosmic ray neutrons that had been slowed down to more or less thermal energies. The flux of these thermal neutrons increases with depth and is highest in the center of a meteorite of roughly one meter radius. Cosmogenic nuclide production by neutron-capture is further discussed in a separate section below.

In summary, Figure 1 illustrates that it is far from trivial to obtain a precise set of production rates for a given sample. Luckily, the preatmospheric radius of stony meteorites rarely exceeded a meter and mostly was less than 40 cm or so. For such bodies, P(^{21}Ne) does not change by more than a factor of ~2 and ~1.5, respectively, at all depths (see also Fig. 4). Hence, an approximate exposure age can normally be estimated even when shielding information is lacking. As an uncertainty of the order of 50% usually is not satisfying, however, either a correction for shielding or a method that largely self-corrects for shielding is required. This will be discussed in the next section. Here we end with an introduction of the most important shielding-sensitive ratios of pairs of cosmogenic noble gas nuclides.

Shielding parameters. The most widely used shielding parameter for stony meteorites is the ratio ^{22}Ne/^{21}Ne of the cosmogenic component (note that we will always talk here about the cosmic-ray-produced fraction of a nuclide, which often has been obtained from measured values after substantial correction for other contributions, such as primordial noble gases; see *Isotopic abundances of cosmogenic noble gases*

subsection). Although P(^{22}Ne) also increases with depth near the surface, it increases somewhat less than P(^{21}Ne), because with a higher flux of secondary neutrons ^{21}Ne production by the reaction ^{24}Mg(n,α)^{21}Ne becomes more important. Therefore, ^{22}Ne/^{21}Ne is largest at the surface of a meteoroid. This is shown in Figure 6, which will be discussed in more detail below. This ratio is also larger in the center of a small meteoroid than in the center of a larger one with the same (relative) abundances of the main target elements producing cosmogenic Ne (mainly Mg, Al, and Si). The ^{22}Ne/^{21}Ne ratio can therefore be used to correct P(^{21}Ne) for shielding (Nishiizumi et al. 1980; Eugster 1988). However, we will see in the next section that this is possible only within certain limits, as the relation between P(^{21}Ne) and ^{22}Ne/^{21}Ne becomes ambiguous at larger shielding. The ratio ^{22}Ne/^{21}Ne also depends somewhat on the Mg/(Mg + Al + Si) ratio. Another often measured shielding-sensitive ratio is ^{3}He/^{21}Ne, which in chondrites positively correlates with ^{22}Ne/^{21}Ne (Eberhardt et al. 1966). However, as cosmogenic ^{3}He and its radioactive precursor ^{3}H ($T_{1/2}$ = 12.3 yr) are prone to diffusive loss, the ^{3}He/^{21}Ne ratio is actually often used instead to recognize meteoroids that may have been heated, e.g., on orbits that brought them relatively close to the Sun. Other shielding indicators in stony meteorites are the ratios ^{78}Kr/^{83}Kr (Eugster et al. 1969; Regnier et al. 1979; Eugster 1988; Lavielle and Marti 1988; Lavielle et al. 1997), and ^{124,126,128}Xe/^{131}Xe (Eugster and Michel 1995; Lavielle et al. 1997), which all correlate positively with ^{22}Ne/^{21}Ne and which also correlate well among one another. The Kr and Xe ratios may be useful in cases where (^{22}Ne/^{21}Ne)$_{cos}$ cannot be determined. In iron meteorites, ^{4}He/^{21}Ne is a useful shielding parameter (Signer and Nier 1960, 1962; Voshage 1978, 1984).

Production systematics

Production systematics of cosmogenic nuclides are studied by different approaches:

(1) survey analyses of many meteorites, e.g., of a specific class;

(2) systematic analyses of several samples from the same meteorite, possibly from different fragments;

(3) nuclide production models that are based on meteorite data, thin-target cross section analyses, or experiments that simulate the cosmic radiation by bombarding thick targets with energetic protons.

In all such studies, multi-nuclide analyses are the rule, and the various approaches are often also combined. Note that a commonly used simplification is to assume that meteoroids had spherical shapes.

Multi-meteorite studies. Perhaps the most straightforward way to determine "average" production rates for meteorites with a certain chemical composition is to analyse a radioactive-stable nuclide pair in a number of meteorites (Herzog and Anders 1971; Nishiizumi et al. 1980; Moniot et al. 1983). Some of these need to have exposure ages comparable to the half-life of the involved radionuclide. Others must have been exposed for much longer, so that the radionuclide activity (number of decays per unit of mass per unit of time) is saturated, i.e., for each freshly made nuclide on average one produced earlier decays. Preferentially, the production rates of the radioactive and stable nuclide should show a similar shielding dependence. Frequently used pairs are ^{26}Al-^{21}Ne, ^{10}Be-^{21}Ne, and ^{53}Mn-^{21}Ne. If all the samples studied are from average-sized meteorites, their radionuclide activities will all have similar values at saturation, and the mean saturation activity is equal to the mean production rate of a radionuclide in the subject meteorite class. The exposure ages of the meteorites in which the radionuclide has not yet reached its saturation level, and hence also the production rate of the stable nuclide can then be determined according to the following equations:

$$T_{exp} = \frac{1}{\lambda} \ln \frac{A_{sat}}{A_{sat} - A_{meas}} \quad , \text{ where } \; A_{sat} > A_{meas} \tag{1}$$

$$P_{stable} = \frac{C_{stable}}{T_{exp}} \tag{2}$$

Here T_{exp} is the exposure age, λ is the decay constant of the radionuclide, and A_{sat} and A_{meas} are the saturation activity and the measured activity of the radionuclide at the time of fall, respectively. P_{stable} and C_{stable} are the production rate and the measured concentration of the stable nuclide, respectively. This method requires that all meteorites considered had a simple exposure history. The production rates deduced in this way are basically the mean values over the last few half-lives of the radionuclide. We will discuss in section *The Cosmic Ray Flux in Time* that this approach can be used to study possible variations of the GCR flux with time.

A further example of the multi-meteorite approach is the work by Eugster (1988), who presents production rates for cosmogenic ^{3}He, ^{21}Ne, ^{38}Ar, ^{83}Kr, and ^{126}Xe as a function of ^{22}Ne/^{21}Ne for various chondrite classes. The data are based on noble gas analyses of a considerable number of ordinary chondrites whose exposure ages were determined by the ^{81}Kr-Kr method, which is largely self-correcting for shielding (see the respective subsection below). The production rate equations and the correction factors F for different chemical compositions are given in Table 1. These factors are based on earlier work in which the relative production rates of each nuclide from various elements or element combinations had been determined either by analysing different minerals from the same meteorite (e.g., Bogard and Cressy 1973) or from model calculations that are discussed below (e.g., Hohenberg et al. 1978). The Eugster formalism has the virtue of yielding a unique production rate for a given value of the routinely determined shielding parameter ^{22}Ne/^{21}Ne. However, as the actual relationship between ^{22}Ne/^{21}Ne and production rate is ambiguous for relatively high shielding, for chondrites the formulas in Table 1 should only be applied for ^{22}Ne/^{21}Ne ratios larger than about 1.08-1.10. They become unreliable for ^{22}Ne/^{21}Ne ratios below about 1.07, as they imply increasing production to very large depth, which is clearly not the case (these limiting ^{22}Ne/^{21}Ne ratios are slightly different for meteorites with higher or lower than chondritic Mg/(Mg + Al + Si) ratios). Furthermore, for very large shielding above some 50 cm or so the trend of ^{22}Ne/^{21}Ne with shielding reverses, as is shown by both model calculations

Table 1. Shielding-corrected production rates in chondrites (Eugster 1988)

	F factors for various chemical classes							
	CI	*CM*	*CO*	*CV*	*H*	*L/LL*	*EH*	*EL*
$P(^{3}He)=F(2.09-0.43\times{}^{22}Ne/^{21}Ne)$	1.01	1.00	0.99	0.99	0.98	1.00	0.97	1.00
$P(^{21}Ne)=1.61F/(21.77\times{}^{22}Ne/^{21}Ne-19.32)$	0.67	0.79	0.96	0.96	0.93	1.00	0.78	0.96
$P(^{38}Ar)=F(0.112-0.063\times{}^{22}Ne/^{21}Ne)$	0.75	0.88	1.03	1.10	1.08	1.00	0.98	0.89
$P(^{83}Kr)=0.0196F/(0.62\times{}^{22}Ne/^{21}Ne-0.53)$	0.71	0.94	1.02	1.13	1.00	1.00	0.75	0.80
$P(^{126}Xe)=F(0.0174-0.0094\times{}^{22}Ne/^{21}Ne)$	0.66	0.93	1.18	1.40	1.00	1.00	0.72	0.72

Production rates P in [10^{-8} cc STP/(g × Myr)] for He, Ne and Ar, and in [10^{-12} cc STP/(g × Myr)] for Kr and Xe (1 cc STP=2.687 × 10^{19} atoms). All values from Eugster (1988), except P(^{38}Ar) for which a ~12% lower value than that given by Eugster (1988) is adopted (Schultz et al. 1991; Graf and Marti 1995). ^{22}Ne/^{21}Ne is the ratio of the cosmogenic component. The shielding correction proposed here is approximately valid only for ^{22}Ne/^{21}Ne > 1.08-1.10, and may fail completely for the rare very large meteorites (see text).

and analyses of the very large Gold Basin meteorite (Masarik et al. 2001; Wieler et al. 2000b; see following subsection). However, such large meteorites are probably very rare, and the $^{22}Ne/^{21}Ne$ shielding parameter in practice is useful in a majority of cases. Note also that more recent studies indicate that P(^{38}Ar) by Eugster (1988) appears to be about 12% too high (Schultz et al. 1991; Graf and Marti 1995). In Table 1 we adopted the lower P(^{38}Ar) values, although the issue is not settled (Eugster et al. 1998b).

Systematic studies on single meteorites and semiempirical models. An example of the second approach to determine production systematics is the study of cosmogenic He, Ne, and Ar, some radionuclides and nuclear tracks in the large chondrite Knyahinya (Graf et al. 1990b) along with follow-up studies that included cosmogenic Kr and Xe (Lavielle et al. 1997) as well as further radionuclides (Reedy et al. 1993; Jull et al. 1994). The main mass of Knyahinya was split in two almost equally sized fragments upon its fall. Fortunately the cut passed very close to the preatmospheric center of the meteorite and the slab included an edge where only a very few cm has been ablated. This happy accident allowed the determination of concentration gradients of the various cosmogenic nuclides as a function of preatmospheric depth. The data were also used to determine the parameters of a semiempiric model of cosmogenic nuclide production (Graf et al. 1990a). This model, based on earlier work by Signer and Nier (1960, 1962) and others, describes production of each nuclide by two depth- and size-dependent terms with only one free parameter each, both of which are independent of shielding. Based on the Knyahinya data and an independently determined exposure age of this meteorite, the model is quite successful in predicting cosmogenic noble gas and radionuclide production rates as a function of depth in chondrites of different sizes (see also figures in Wieler et al. 1996). Similar semiempirical models have been used to describe nuclide production in stony-iron or iron meteorites (e.g., Honda 1988). Voshage (1978, 1984) combined noble gas data with determinations of the very long-lived cosmogenic radionuclide ^{40}K ($T_{1/2}$ = 1.25 Gyr) in iron meteorites (see also *The Cosmic Ray Flux in Time* section).

Many further comprehensive studies on single meteorites have either contributed to our understanding of cosmogenic nuclide production systematics or the exposure histories of the studied meteorites. Some examples are the investigations on Grant (Signer and Nier 1960, 1962; Graf et al. 1987), Keyes (Wright et al. 1973), St. Severin (Schultz and Signer 1976; Lavielle and Marti 1988), Jilin (Begemann et al. 1996; Heusser et al. 1996 and references therein), Chico (Garrison et al. 1992), Bur Gheluai (Vogt et al. 1993); Canyon Diablo (Heymann et al. 1966; Michlovich et al. 1994), and Gold Basin (Kring et al. 2001; Wieler et al. 2000b).

Physical models. Much progress has also been made in modeling cosmogenic nuclide production in meteorites based essentially only on physical principles and without using any free parameters except for the absolute cosmic ray flux. These models simulate all the processes relevant for particle production and transport using Monte Carlo techniques (Masarik and Reedy 1994; Masarik et al. 2001; Leya et al. 2000a, Leya et al. 2001b and references therein). The basic equation underlying these models is (e.g., Leya et al. 2000a).

$$P_j(R,d,M) = \sum_{i=1}^{N} c_i \frac{N_A}{A_i} \sum_{k=1}^{3} \int_0^{\infty} \sigma_{j,i,k}(E) \times J_k(E,R,d,M) dE \qquad (3)$$

where $P_j(R,d,M)$ is the production rate of nuclide j as a function of the meteoroid radius R, sample depth d, and the solar modulation parameter M (this parameter is a measure for the reduction of the GCR particle flux by the Sun's magnetic field; see also Niedermann 2002). The first sum goes over all target elements i, while the index k in the second sum represents the reaction particle type (primary or secondary proton, secondary neutron). N_A is Avogadro's number, A_i the mass number (in amu) of the target element i, c_i the

abundance of element i (in g/g). $\sigma_{j,i,k}(E)$ is the excitation function for the production of nuclide j from element i by reactions induced by particles of type k, and $J_k(E,R,d,M)$ is the differential flux density of particle type k, which depends on the energy E of the reacting particles (as well as on R, d, and M). Note that the primary GCR intensity is assumed to be constant in time (see also *The Cosmic Ray Flux in Time* section). Note also that the models by Leya and coworkers and Masarik and coworkers take into account primary and secondary alpha particles only approximatively, by multiplying production rates from Equation (3) by a factor of 1.55 (the 12% alpha particles in the GCR have 55% as much mass—and hence energy—as the 87% GCR protons).

Equation (3) shows that the most critical ingredients for such models are the numerous excitation functions needed. The data base for proton-induced reactions is fairly complete for most relevant noble gas nuclides as well as for most of the important radionuclides. An important exception is ^{36,38}Ar production from Ca, for which cross sections are still based only on theoretical nuclear models (e.g., Blann 1971). Measured cross sections for neutron-induced reactions are, however, very scarce (e.g., Sisterson et al. 2001). This is a serious problem because secondary neutrons usually dominate the cosmogenic nuclide production. Leya (1997) and Leya and Michel (1997) therefore derived excitation functions for neutron-induced reactions with the data from five thick-target simulation experiments, where stony or iron spheres of various radii and filled with a large number of target foils were isotropically irradiated by energetic protons (Michel et al. 1986; Leya et al. 2000b and references therein). Neutron excitation functions were derived for all reactions where the proton-induced production could be reliably calculated, based on their known excitation functions, and so subtracted.

Figures 2-6 present some important results from the models by Leya et al. (2000a) and Masarik et al. (2001). Figure 2 shows that both models do reproduce the measured ^{21}Ne depth profile in Knyahinya well, and hence can be expected to reliably predict nuclide production in meteorites of a wide range of sizes. Remarkably, secondary neutrons contribute about two thirds to the total ^{21}Ne production at the surface and this fraction increases to 85% near the center. This illustrates the importance of reliable neutron cross section data. Figures 3 and 4 show the ^{3}He and ^{21}Ne production rates, respectively, in the two most abundant meteorite classes, the H and L chondrites, as a function of depth and size. As noted above, for average-sized meteorites ($R < 40$ cm), production rates vary within only about a factor of 1.5. On the other hand, for the Gold Basin chondrite with its preatmospheric radius of perhaps 3 m, nuclide concentrations vary by more than an order of magnitude (Kring et al. 2001; Wieler et al. 2000b). This meteorite is almost represented by the lines denoting an infinite radius (2π).

Figure 5 shows P(^{21}Ne) values versus the ^{22}Ne/^{21}Ne ratio for objects of various sizes and samples of various depths according to calculations by Leya et al. (2001a). Also shown is the empirical curve according to Eugster (1988) that is given in Table 1. The Figure shows that the relation between P(^{21}Ne) and ^{22}Ne/^{21}Ne is more or less unique only for ^{22}Ne/^{21}Ne ≥ 1.13, i.e., for meteorites with radii less than some 15 cm or for near-surface samples of somewhat larger bodies. In more heavily shielded samples, P(^{21}Ne) may differ by up to a factor of 2 at a given ^{22}Ne/^{21}Ne. However, this large spread is only observed for objects with radii above ~85 cm (filled symbols), which fortunately are rare. For more common sizes and mean values of ^{22}Ne/^{21}Ne of 1.08-1.14, the model predictions agree quite well with the Eugster (1988) calibration curve. At lower shielding, the empirical calibration curve runs parallel to the model results, although with an offset of up to 30%. In summary, Figure 5 indicates that the shielding-corrected P(^{21}Ne) values according to Eugster (1988) are usually correct to within some ± 15% for average

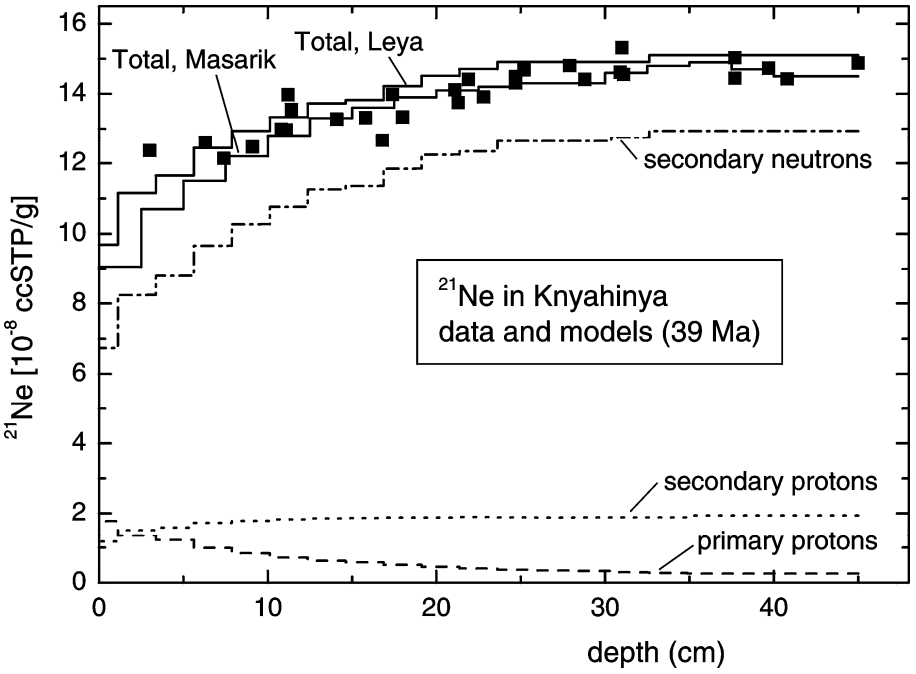

Figure 2. Comparison of measured (squares) and modelled (solid lines) ^{21}Ne concentrations in the L/LL chondrite Knyahinya. The measured data are from Graf et al. (1990b), and the two model curves from Leya et al. (2000a) and Masarik et al. (2001). Both models assume a radius of Knyahinya of 45 cm and an exposure age of 39 Myr. Also shown are the individual contributions by primary protons and secondary protons and neutrons (Leya et al. 2000a). Note that even at the surface, most of the ^{21}Ne is produced by secondary particles.

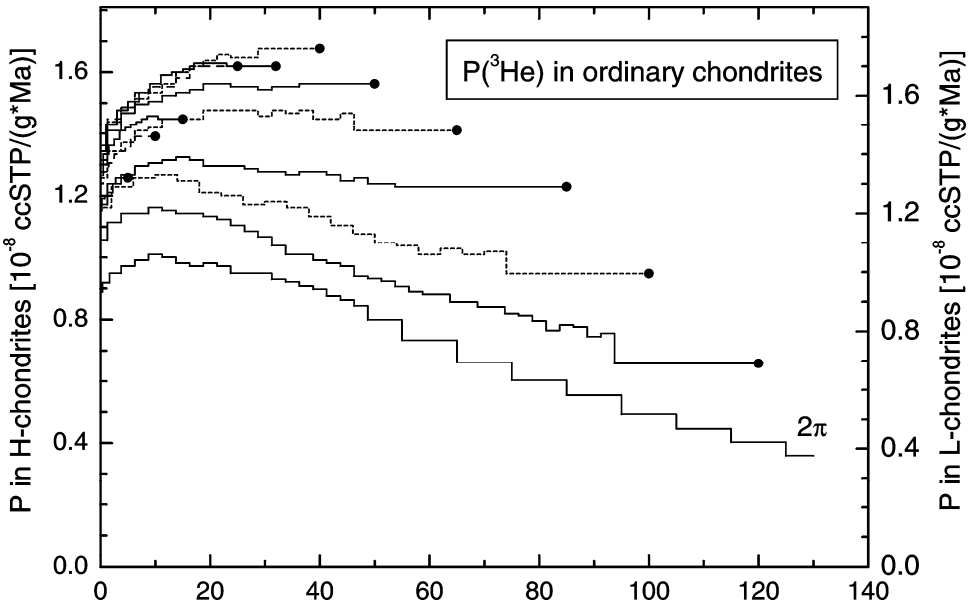

Figure 3. GCR-induced production rates of ^{3}He in ordinary chondrites of classes H (left ordinate) and L (right ordinate). For LL chondrites, all values are 2% larger than those of L chondrites. The curves represent meteoroids with radii of between 5 and 120 cm. Also included is a depth profile on an infinitely large flat body (2π). Model calculations are from Leya et al. (2000a) and updates (I. Leya, pers. comm. 2001).

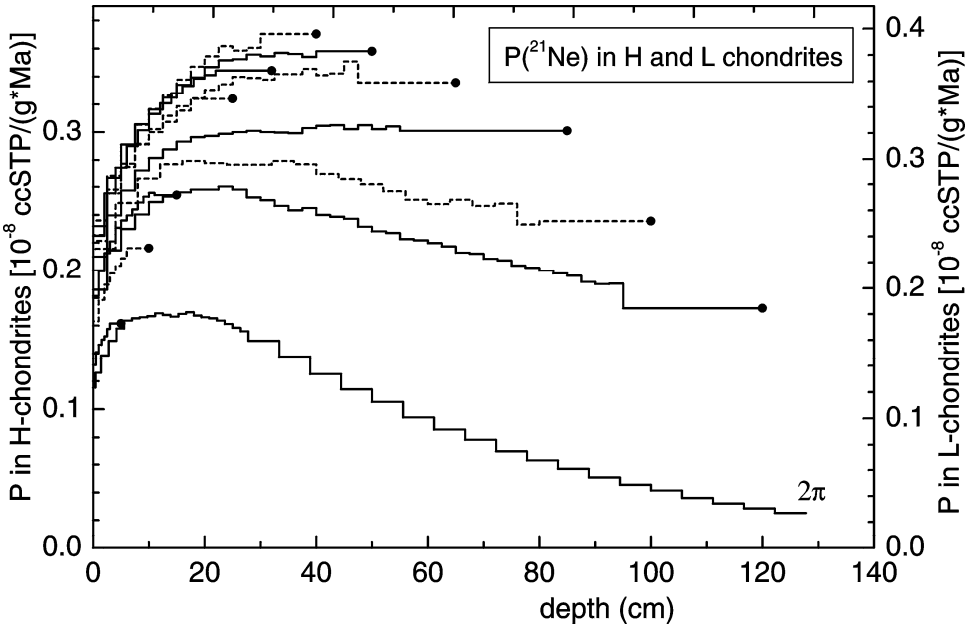

Figure 4. Same as Fig. 3 but for ^{21}Ne. For LL chondrites, the L-scale on the right ordinate has to be multiplied by 1.02. Data from Leya et al. (2000a).

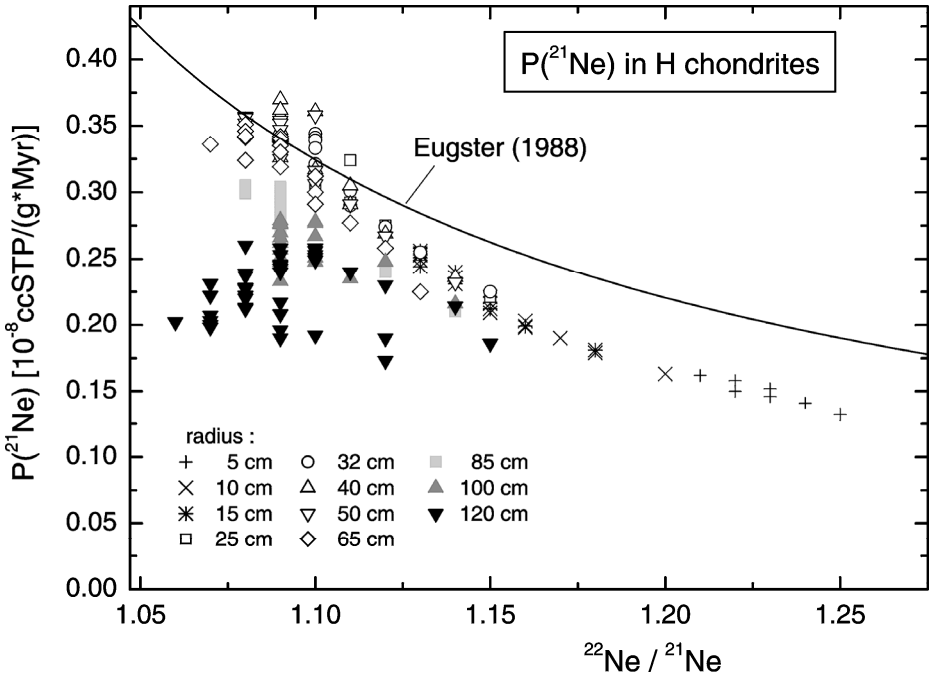

Figure 5. The symbols show the GCR production rate of ^{21}Ne as a function of the shielding parameter ^{22}Ne/^{21}Ne in H chondrites of various radii and samples from variable depths, calculated according to Leya et al. (2001a). Also shown is the empirical relation between P(^{21}Ne) and ^{22}Ne/^{21}Ne according to Eugster (1988). The model data show that only for ^{22}Ne/^{21}Ne $\geq$ 1.13 there exists an essentially unequivocal P(^{21}Ne) value. At lower ^{22}Ne/^{21}Ne values, P(^{21}Ne) varies by up to twofold at a given ^{22}Ne/^{21}Ne. Nevertheless, for meteorite radii not larger than ~50 cm, the Eugster (1988) relation is in agreement with the model results to within ±15% for 1.08 < ^{22}Ne/^{21}Ne < 1.14. It is unclear whether the physical model or the empirical correlation describes the data better for ^{22}Ne/^{21}Ne > 1.13.

shielding ($^{22}Ne/^{21}Ne$ = 1.08-1.13). So far it is unclear whether the physical model or the empirical correlation predicts P(^{21}Ne) more accurately for $^{22}Ne/^{21}Ne > 1.13$, as samples with such low shielding with independently calibrated exposure ages are rare.

Figure 6 shows the utility and the ambiguities of using $^{22}Ne/^{21}Ne$ as a shielding parameter in yet another way. The model by Masarik et al. (2001) reproduces this ratio very well for meteorites of the size of Knyahinya (R ~45 cm). However, in very large objects, this ratio increases with shielding, such that, e.g., a sample from the center of a R = 2 m chondrite has the same $^{22}Ne/^{21}Ne$ value as a sample from 5 to 10 cm below the surface of Knyahinya.

Elemental production rates. The relationships shown in Figures 2-6 constrain production rates for meteorites with the chemical composition of ordinary chondrites, but they are not directly applicable to other meteorite classes with distinctly different concentrations of the relevant target elements. To do this, production rates from each major target element are needed, and these are also provided by the models. Table 2 is a much abbreviated version of lists of elemental production rates of ^{3}He, ^{21}Ne, and $^{22}Ne/^{21}Ne$ for meteoroids of various sizes provided by Leya et al. (2000a) for Ne and I. Leya (pers. comm. 2001) for He, respectively. Also given are ^{38}Ar production rates from Fe and Ni (Leya et al. 2001b). Production of ^{38}Ar from Ca, the major target element in stony meteorites, has not yet been calculated with the "Hannover model" developed by R. Michel, I. Leya and coworkers, because of the lack of experimentally determined cross sections. We therefore reproduce in Table 2 the older ^{38}Ar values from Ca (and other elements) presented by Hohenberg et al. (1978) for infinitely large bodies (2π exposure geometry), although the accuracy of these values is unclear. Elemental production rates for other noble gases are also given by Regnier et al. (1979) and Reedy (1981).

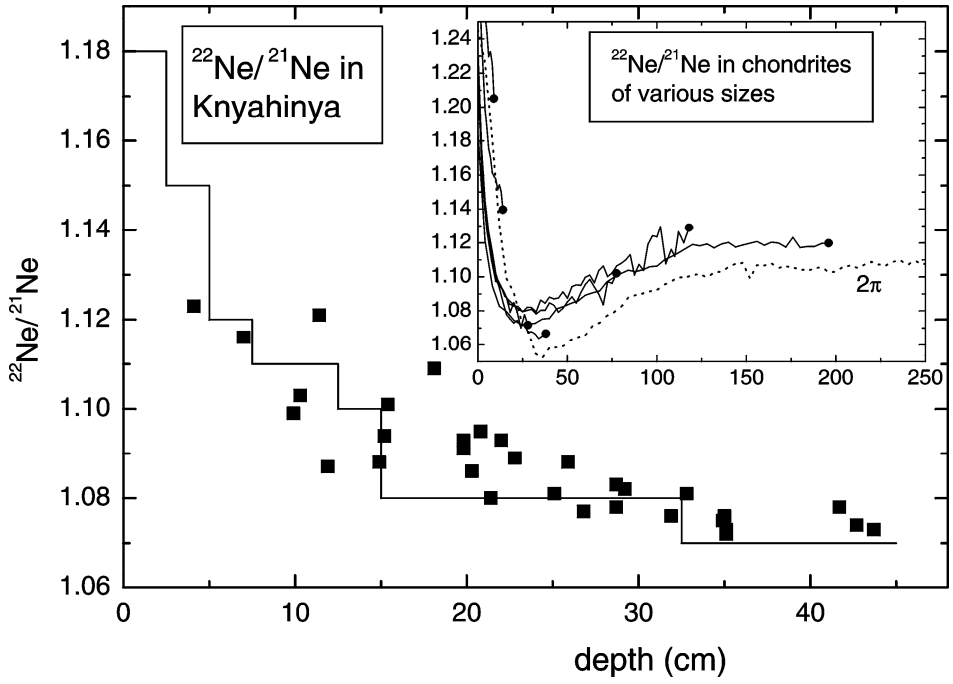

Figure 6. In the main panel, the $^{22}Ne/^{21}Ne$ ratio predicted by the model of Masarik et al. (2001) is compared with data from Knyahinya samples from known preatmospheric depths (Graf et al. 1990b). The inset shows the modelled ratios for various meteorite radii and a 2π irradiation. At depths below ~50 cm, $^{22}Ne/^{21}Ne$ increases again. Therefore, the same $^{22}Ne/^{21}Ne$ ratio corresponds to widely different depths, which illustrates the ambiguity of this ratio as a shielding index in very large meteorites.

Table 2. Elemental production rates of cosmogenic He, Ne, and Ar in meteorites

radius/ depth	*^{3}He*					*^{21}Ne*					*^{22}Ne/^{21}Ne*				*^{38}Ar*			
	O	*Mg*	*Al*	*Si*	*Fe*	*Mg*	*Al*	*Si*	*Ca*	*Fe*	*Mg*	*Al*	*Si*	*Ca*	*Ca*	*Ti*	*Fe*	*Ni*
5,s	148	113	124	138	86.6	53.2	32.6	25.2	8.57	2.03	1.290	1.188	1.197	1.256			7.47	6.54
5,c	166	124	130	143	89.0	69.0	37.8	28.8	8.77	1.99	1.200	1.224	1.197	1.236			7.43	6.58
10,s	163	125	130	142	88.2	70.2	37.4	28.8	8.69	1.97	1.191	1.228	1.190	1.234			7.39	6.50
10,c	190	144	139	149	90.8	98.7	45.9	34.9	8.89	1.86	1.091	1.265	1.187	1.197			7.23	6.41
15,s	170	132	131	143	87.3	80.4	39.6	30.6	8.53	1.88	1.152	1.260	1.187	1.223			7.19	6.33
15,c	202	158	139	150	87.2	121.0	49.9	38.0	8.40	1.66	1.054	1.325	1.185	1.175			6.66	5.89
25,s	186	148	135	147	86.8	102.7	44.7	34.6	8.36	1.75	1.095	1.309	1.184	1.200			6.78	6.01
25,c	232	188	149	158	88.2	159.2	59.3	45.5	8.32	1.46	1.020	1.377	1.188	1.127			6.17	5.52
40,s	188	152	132	144	82.8	111.7	45.5	35.6	7.88	1.60	1.076	1.339	1.176	1.185			6.33	5.60
40,c	246	205	148	156	82.7	184.3	65.0	51.2	7.63	1.14	1.002	1.413	1.151	1.075			5.32	4.79
65,s	173	144	120	133	74.5	108.0	41.8	33.2	7.02	1.41	1.071	1.369	1.174	1.179			5.60	4.95
65,c	210	180	119	127	62.0	171.7	53.6	43.4	5.44	0.69	0.969	1.470	1.159	1.022			3.63	3.22
100,s	161	135	112	123	68.1	104.3	39.2	30.9	6.33	1.26	1.066	1.388	1.189	1.180			5.08	4.47
100,c	138	130	78.5	86.2	38.7	120.6	36.5	30.2	3.20	0.37	1.020	1.537	1.150	0.994			2.00	1.80
2π, 0	118	97	90	100	58	59.9	24.7	19.9	5.40	1.31	1.061	1.190	1.224	1.235	*61*	*11.8*	4.42	3.96
2π, 40	146	113	86	90	49	93.1	34.3	27.1	4.50	0.73	0.927	1.175	1.196	1.100	*113*	*11.1*	3.14	2.83
2π, 100	127	98	66	70	35	83.1	28.9	23.7	3.06	0.37	0.896	1.188	1.163	1.027	*103*	*7.48*	1.96	1.75
2π, 200	83	64	40	43	20	52.7	17.7	15.0	1.63	0.16	0.905	1.208	1.145	0.978	*72*	*3.91*	0.97	0.78
2π, 500	15	12	7	8	3	9.9	3.0	2.8	0.22	0.01	0.917	1.255	1.116	0.908	*12.0*	*.42*	0.12	0.10

Production rates [in 10^{-10} ccSTP/(g × Ma)] according to model calculations (1 ccSTP = 2.687×10^{19} atoms). Given are values for the surface (subscript s) and the center (subscipt c), respectively, of meteorites with radii between 5 and 100 cm. The lowermost 5 rows give the values for an infinitely large body (2π irradiation) at depths between 0 and 500 g/cm^2. Most data are from I. Leya and coworkers (^{3}He: I. Leya, pers. comm. 2001; ^{21}Ne (4π): Leya et al. 2000a; Ne (2π): Leya et al. 2001; ^{38}Ar from Fe and Ni: Leya et al. 2001). ^{38}Ar from Ca and Ti (2π) values are from Hohenberg et al. 1978. These values should not be compared straightforwardly with the respective ^{38}Ar data from Fe and Ni by Leya et al. 2001, because the latter values are considerably higher than P(^{38}Ar) from Fe and Ni also reported by Hohenberg et al. 1978. ^{22}Ne/^{21}Ne from Fe as target not given, because P(^{22}Ne) from Fe reported by Leya et al. (2000a, 2001) is unreliable. This table is a summary of much more extended data sets given in the original publications.

The matrix effect. When calculating a production rate for a sample with a given chemical composition by multiplying the elemental production rates times the fractional abundance of the respective target element and summing over all relevant elements, one ignores a possible dependence of elemental production rates on the overall chemical composition of a meteorite. This so-called matrix effect can arise because particle fluxes and spectra are a function of the chemical composition of the target. For example, the matrix effect is expected to be important for silicate inclusions in stony-iron meteorites, where the high Fe concentrations lead to an enhanced flux of secondary neutrons relative to stony meteorites (Begemann and Schultz 1988; Masarik and Reedy 1994). The matrix effect will be particularly pronounced for nuclides largely produced by relatively low-energy neutrons, e.g., ^{21}Ne from ^{24}Mg and ^{38}Ar from Ca. Albrecht et al. (2000) showed that ^{21}Ne production rates in silicates from mesosiderites on average are some 60% higher than would be expected for samples with the same composition but in a silicate-only matrix. This result is in agreement with the model calculations by Masarik and Reedy (1994). For stony meteorites of variable composition the matrix effect is generally expected to be < 10%, however, an exception being ^{38}Ar production from Ca, which is several ten percent lower in eucrites and aubrites compared to chondrites (Masarik and Reedy 1994).

Production rate ratios P(^{10}Be)/P(^{21}Ne) and P(^{26}Al)/P(^{21}Ne). Because of the ambiguity of the parameter ^{22}Ne/^{21}Ne, other methods for deducing shielding-corrected production rates are often useful. These methods operate with a radioactive and a stable nuclide pair that have production rate ratios that can be assumed to depend only weakly on the irradiation conditions. We already mentioned the systems ^{10}Be-^{21}Ne, ^{26}Al-^{21}Ne, and ^{53}Mn-^{21}Ne, which can be used not only to deduce average production rates as shown above, but in principle also to derive a shielding-corrected ^{21}Ne production rate for an individual sample.

Based on the Knyahinya data, Graf et al. (1990a) proposed the following relations for L chondrites (in atoms/atom):

$$\frac{P(^{10}Be)}{P(^{21}Ne)} = (0.140 \pm 0.001) + (0.02 \pm 0.05) \times \left(\frac{^{22}Ne}{^{21}Ne} - 1.11 \right) \quad (4)$$

$$\frac{P(^{26}Al)}{P(^{21}Ne)} = (0.37 \pm 0.02) - (0.4 \pm 0.7) \times \left(\frac{^{22}Ne}{^{21}Ne} - 1.11 \right) \quad (5)$$

Note that the two production rate ratios P(^{10}Be)/P(^{21}Ne) and P(^{26}Al)/P(^{21}Ne) are given as functions of ^{22}Ne/^{21}Ne and are thus basically also subject to the reservations on the reliability of this shielding parameter. However, the dependence of P(^{10}Be)/P(^{21}Ne) on ^{22}Ne/^{21}Ne in Equation (4) is actually very weak, which reflects the fact that the ratio ^{10}Be/^{21}Ne is nearly constant over the entire range of shielding represented by the Knyahinya samples. The pair ^{10}Be-^{21}Ne therefore offers a way to determine shielding-corrected exposure ages in chondrites (Eqn. 4), if ^{10}Be can be assumed to be saturated, i.e., for exposure ages above ~6 Myr. A word of caution is necessary, however. In contrast to the model of Graf et al. (1990a), that by Leya et al. (2000a) predicts P(^{10}Be)/P(^{21}Ne) in chondrites to depend substantially on the ratio ^{22}Ne/^{21}Ne. If so, ^{10}Be-^{21}Ne ages are correct only to within the limits imposed by the reliability of ^{22}Ne/^{21}Ne as shielding indicator. Leya et al. (2000a) estimate that for ^{22}Ne/^{21}Ne < 1.10 ^{10}Be-^{21}Ne ages are ambiguous to within ±15%.

In iron meteorites this ambiguity does not appear to exist. Both data and models show that the ratio P(^{10}Be)/P(^{21}Ne) is constant over a wide range of shielding. Lavielle et

al. (1999a) derive a P(^{10}Be)/P(^{21}Ne) value of 0.55, in perfect agreement with the model-based value by Leya et al. (2000a), which is essentially independent on shielding for all meteorites with radii not larger than one meter. Graf et al. (1987) had deduced a P(^{10}Be)/P(^{21}Ne) ratio of 0.772±0.05 with data from the Grant iron meteorite, by adopting an exposure age derived with the ^{40}K-^{41}K method. This ratio is 40% higher than that published by Lavielle et al. (1999a), which is based on the ^{36}Cl-^{36}Ar age of Grant and another iron meteorite. As Cl-Ar and K-K ages of iron meteorites differ systematically by ~40%, probably because the cosmic ray intensity has changed with time (see *The Cosmic Ray Flux in Time* section), the production rate ratios P(^{21}Ne)/P(^{10}Be) given by Graf et al. (1987), Lavielle et al. (1999a), and Leya et al. (2000a) therefore all agree very well. If we adopt the ^{36}Cl-^{36}Ar age scale, a ^{10}Be-^{21}Ne age of iron meteorites can therefore be calculated by

$$T_{exp} = \left(\frac{^{21}\mathrm{Ne}}{\mathrm{P}(^{10}\mathrm{Be})} \right) \times 0.55 \tag{6}$$

where ^{21}Ne is the concentration in atoms per unit of mass and P(^{10}Be) the production rate in atoms per unit of mass per unit of time.

In iron meteorites, the P(^{26}Al)/P(^{21}Ne) ratio also appears to be rather insensitive to shielding. Leya et al. (2000a) predict an essentially constant value of 0.45, somewhat higher that that of 0.38 proposed by Hampel and Schaeffer (1979), which is based on the ^{36}Cl-^{36}Ar age scale. The mean value of 0.56 by Graf et al. (1987) (based on the ^{40}K-^{41}K age scale) is again 25-47% higher than the other two values. However, in contrast to the model prediction (Leya et al. 2000a), the measured P(^{26}Al)/P(^{21}Ne) in Grant increases somewhat with increasing shielding (Graf et al. 1987).

The ^{36}Cl-^{36}Ar, ^{129}I-^{129}Xe, and ^{81}Kr-Kr methods. These methods do not involve ^{22}Ne/^{21}Ne, and are thus self-correcting for shielding in a more strict sense than the ^{10}Be-^{21}Ne method in chondrites. The ^{36}Cl-^{36}Ar pair has the advantage that in metallic Fe-Ni samples most of the ^{36}Ar is produced through its radioactive precursor ^{36}Cl, and hence the production rate ratio P(^{36}Ar)/P(^{36}Cl) is undoubtedly essentially shielding-independent. One advantage of the ^{81}Kr-Kr technique is that both radioactive and stable nuclide are isotopes of the same element krypton, so only an isotopic ratio measurement is needed. Note, however, that these methods also will yield erroneous ages if the assumption of a single stage exposure history of the studied sample is violated.

Lavielle et al. (1999a) and Graf et al. (2001) give values for P(^{36}Cl)/[γP(^{36}Cl) + P(^{36}Ar$_{direct}$)] of 0.84±0.04 for Fe and 0.78±0.03 for Ni. These values should be shielding-independent for production by both protons and neutrons. The coefficient $\gamma = 0.981$ is the branching ratio for the decay of ^{36}Cl into ^{36}Ar. With an average Ni concentration of 9% in chondritic metal, the ^{36}Cl-^{36}Ar age can be calculated by

$$T_{exp} = 0.363 * \left(\frac{^{36}\mathrm{Ar}_{cos}}{^{36}\mathrm{Cl}} \right) \tag{7}$$

if [atoms per gram] are used as units for the concentrations of cosmogenic (subscript cos) ^{36}Ar and ^{36}Cl, or

$$T_{exp} = 427 * \left(\frac{^{36}\mathrm{Ar}_{cos}}{^{36}\mathrm{Cl}} \right) \tag{8}$$

using [10^{-8} ccSTP/g] for ^{36}Ar and [dpm/kg] for ^{36}Cl.

Begemann et al. (1976), Leya et al. (2000a) and Albrecht et al. (2000) give coefficients of 425, 433 and 430, respectively, for Equation (8). Whereas ^{36}Cl-^{36}Ar ages are thus basically very reliable, they are quite difficult to determine, because very high-purity metal separates are required to avoid contamination with ^{36}Cl and ^{36}Ar from silicate impurities (e.g., Graf et al. 2001). Also, ^{36}Cl and ^{36}Ar have to be analyzed on two different, often small aliquots. Therefore, rather few ^{36}Cl-^{36}Ar exposure ages have been reported so far, although the method is becoming increasingly popular.

Another potentially interesting method where the stable cosmogenic noble gas nuclide is predominantly produced through a radioactive precursor is the live-^{129}I-^{129}Xe method (Marti et al. 1986). All cosmogenic ^{129}Xe produced from Te will have gone through ^{129}I (half-life 15.7 Myr). For samples where ^{129}Xe contributions from Ba can be corrected for (using ^{124,126}Xe) and for which ^{129}Xe contributions from extinct ^{129}I from the early solar system are of no concern, this system is ideal in being self-correcting for both shielding and variable Te abundance. Marti et al. (1986) determined the exposure age of the big Cape York iron meteorite with the live-^{129}I-^{129}Xe couple in troilite inclusions. Otherwise, the method has not been widely applied so far, but as ^{129}I analyses by accelerator mass spectrometry are becoming routine, it should prove very useful to study cosmic ray flux variations over timescales of a few ten million years.

The ^{81}Kr-Kr technique was proposed by Marti (1967). Cosmogenic Kr is mainly produced from the target elements Rb, Sr, Y, and Zr. ^{81}Kr has a half-life of 229,000 yrs. Marti and Lugmair (1971) observed that the isotopic ratios of cosmogenic Kr vary systematically in Apollo 12 lunar rocks, due to variable shielding. They observed the following relations (all Kr concentrations or isotopic ratios refer to the spallation Kr component):

$$P(^{81}\mathrm{Kr}) / P(^{83}\mathrm{Kr}) = 0.95\left(\frac{^{80}\mathrm{Kr}+^{82}\mathrm{Kr}}{2\times^{83}\mathrm{Kr}}\right) \quad (9)$$

and

$$P(^{81}\mathrm{Kr}) / P(^{83}\mathrm{Kr}) = 1.262\frac{^{78}\mathrm{Kr}}{^{83}\mathrm{Kr}} + 0.381 \quad (10)$$

These relations allow determination of a shielding-corrected exposure age based on a single Kr analysis The factor 0.95 in Equation (9) represents the isobaric fraction yield of ^{81}Kr (Marti 1967). Note that this value has recently been redetermined to ~0.92 for chondritic abundances of the relevant target elements (B. Lavielle, pers. comm. 2001). The second relation is insensitive to ^{80}Kr and ^{82}Kr from neutron capture on Br, which is present in relatively large or Br-rich meteorites (see next section). Note, that these relations are strictly valid only for samples which have the same relative abundances of the major target elements as Apollo 12 rocks. For example, Apollo 11 samples, which have ~2-3 times higher Zr/Sr ratios than Apollo 12 samples, have a P(^{81}Kr)/P(^{83}Kr) that is slightly higher at a given ^{78}Kr/^{83}Kr value than predicted by Equation (10) (Lugmair and Marti 1971). However, the difference is only about 1-3%. Moreover, Finkel et al. (1978) showed that the Kr spallation systematics derived from Apollo 12 samples are also valid for the two chondrites San Juan Capistrano and St. Severin, apparently because Apollo 12 rocks and chondrites have rather similar Zr/Sr ratios (although very different Rb/Sr ratios, Rb contributing substantially to Kr production in chondrites but not in lunar samples). Equations (9) and (10) are thus also widely used today for meteorites. Eugster (1988) presented a correlation between P(^{81}Kr)/P(^{83}Kr) and ^{22}Ne/^{21}Ne, for ordinary chondrites, but from the only available ^{81}Kr depth profile in Knyahinya it is unclear whether this relation holds for low shielding (Lavielle et al. 1997). The ^{81}Kr-Kr method has the

disadvantage of often not being very precise, both because of the low abundance of ^{81}Kr and because large corrections for non-cosmogenic Kr are often required.

An important caveat is that all procedures for deducing production rates discussed above assume a single-stage exposure. In other words, it is assumed that a meteorite was ejected from its parent body from at least several meters depth, where it had been completely shielded from the GCR, and then travelled to Earth without ever changing its shape by a further collision or by space erosion (see *Complex Exposure Histories* section). Only in this case is the present-day activity of a radionuclide a good measure for the production rate of a stable nuclide, as the radionuclide concentration depends only on the shielding of the sample during the past few half-lives, whereas the stable nuclide has been accumulating during the entire exposure of the sample to cosmic rays. However, we will see in the *Complex Exposure Histories* section that for a fairly high fraction of all meteorites this requirement of a single exposure stage is probably not fulfilled. Complex exposures may well go unnoticed, e.g., if a single noble gas analysis on a single sample has been carried out only.

A factor further limiting the accuracy of production rates is a possible change in the mean GCR flux over the timescales of interest. We will discuss in section *The Cosmic Ray Flux in Time* that such variations on a million-year scale appear to be modest but that the mean flux during the last few or few ten million years probably has been some 40 to 50% higher than the mean over the past 1-2 Gyr. The resulting additional uncertainty of exposure ages is often only a minor concern, however. This is because one is often more interested in whether exposure ages of different meteorite classes cluster at certain values rather than in the absolute position of such clusters. It needs, however, to be taken into account if ages based on production rates derived from different nuclide systems are compared with each other, particularly for iron meteorites (see the respective subsection below).

In summary, production rates of cosmogenic nuclides in meteorites have quite a variable level of accuracy and reliability. In general, the more nuclides that are determined on the same sample and the more samples that are measured from the same meteorite, the higher will be our confidence in a stated exposure age. A single age determination will usually not be more accurate than to within 15-20%, with the probable exception of ^{36}Cl-^{36}Ar ages, which may have a precision of better than 10%. Uncertainties may even be considerably larger than 20%, e.g., if an unusually heavy shielding is not recognized. On the other hand, we will see below that the accuracy that is presently achieved generally is good enough to study the history of meteorites as small bodies in space and collisional processes on parent bodies.

Cosmogenic noble gases produced by capture of low-energy neutrons

So far, we have mainly discussed production of cosmogenic nuclides by neutrons or protons with energies high enough (tens of MeVs or higher) to break up a target nucleus. The resulting cosmogenic nuclide (commonly referred to as "spallation product") usually has a lower mass than the original target. In contrast to this, target nuclei may also capture secondary cosmic ray neutrons which have already been slowed down to much lower energy without having yet interacted with a nucleus. These are so-called thermal (<0.6 eV) or epithermal (up to hundreds of eV) neutrons. We mentioned in the *Introduction* that several isotopes of Cd, Sm and Gd have a cross section high enough so that capture of thermal or epithermal neutrons induces measurable shifts in their isotopic composition in samples exposed to GCR. We also mentioned ^{60}Co, a nuclide predominantly produced by thermal neutron capture on ^{59}Co. Here we discuss how several stable noble gas nuclides are also efficiently produced by slow neutron-capture reactions so that sometimes a sizeable fraction of the respective nuclide may be produced

by this pathway, although this is unfortunately often difficult to quantify. The most important of these nuclides are ^{36}Ar, ^{80,82}Kr, and ^{128,131}Xe.

The flux of thermal and epithermal neutrons peaks at larger depths (in large objects roughly around 200 g/cm^2) than the depth of maximum production of nuclides made by particles of higher energy (Eberhardt et al. 1963; Lingenfelter et al. 1972; Spergel et al. 1986; Nishiizumi et al. 1997b). Nuclides produced by thermal or epithermal neutrons are therefore potentially very useful for studying cosmic ray interactions at relatively high shielding. For example, high levels of neutron-capture products in a meteorite otherwise thought to have been of "average" preatmospheric size would reveal a complex exposure history, since the neutron-capture nuclides would have been acquired on the parent body or in a larger precursor meteoroid (see *Complex Exposure Histories* section*)*. Neutron-capture products have also been widely used to study the GCR irradiation history of the lunar regolith (see Wieler et al. 2002). Bogard et al. (1995) give an overview of applications of neutron-capture-produced nuclides in extraterrestrial samples.

The noble gases are themselves much too rare to serve as significant neutron-capture targets. For this reason, neutron-capture-produced noble gas isotopes must have a radioactive precursor formed from another element. For example, neutron-capture-produced ^{36}Ar (^{36}Ar$_n$) results from the reaction ^{35}Cl(n,γ)^{36}Cl(β^-)^{36}Ar. Similarly, ^{80}Kr and ^{82}Kr are produced from ^{79}Br and ^{81}Br through ^{80,82}Br (Lugmair and Marti 1971). The most important neutron-capture-produced isotope of Xe is ^{131}Xe from ^{130}Ba (with intermediate products ^{131}Ba and ^{131}Cs). This is a particularly interesting system because Ba is also the major target element for the production of cosmogenic Xe by high-energy reactions, so ratios such as ^{131}Xe/^{126}Xe provide a measure for the depth of irradiation virtually independent of the chemical composition of a sample (Eberhardt et al. 1971). ^{128}Xe from ^{127}I may also be detectable, e.g., in calcium-aluminum-rich inclusions in Allende (Göbel et al. 1982) or near the surface of lunar dust grains where volatile iodine had been concentrated (Pepin et al. 1995). These examples show that sometimes care needs to be taken to distinguish neutron-capture products from other contributions like potential nucleosynthetic anomalies or implanted solar wind Xe.

A major problem limiting the applicability of neutron-capture-produced noble gases is that other noble gas components often hamper a quantitative determination of the neutron-capture component. This is a particular problem in the case of ^{36}Ar. Essentially every meteorite contains cosmogenic Ar produced by high-energy spallation (^{36}Ar/^{38}Ar ~ 0.65), and most stony meteorites contain primordial Ar (^{36}Ar/^{38}Ar ~ 5.3) or some atmospheric Ar with essentially the same ^{36}Ar/^{38}Ar ratio as the primordial component. As long as only these components have to be taken into account, the concentrations of cosmogenic ^{36}Ar and ^{38}Ar can be deduced unambiguously, but this cannot be done any more when ^{36}Ar$_n$ may also possibly be present. To firmly prove the presence or absence of ^{36}Ar$_n$ in a meteorite is therefore generally quite a formidable task, involving e.g., Ar release in several temperature steps and combining such measurements with analyses of other neutron-capture nuclides (Bogard et al. 1995) and/or analyses of multiple samples from the same meteorite (e.g., Welten et al. 2001a). Even then, it may still be difficult to quantitatively determine the concentration of the neutron-capture-produced ^{36}Ar, so that only lower and upper limits may be estimated. In practice, this often leads researchers to neglect the possible presence of ^{36}Ar$_n$ even in cases where this may not be warranted. Bogard et al. (1995) showed that ^{36}Ar$_n$ accounts for perhaps more than half of the total (cosmogenic and trapped) ^{36}Ar in the large chondrite Chico, and they discuss observations indicating the presence of ^{36}Ar$_n$ in several other large meteorites or meteorites with a known complex exposure history. They note that this is not a surprise but rather is to be expected. Therefore, neglecting this component may often compromise

the determination of conventional ^{38}Ar exposure ages. This is because the measured ^{38}Ar essentially must always be corrected for primordial or atmospheric Ar, as just mentioned, and this correction will be too large if the $^{36}Ar_n$ is erroneously viewed to be primordial or atmospheric (e.g., Welten et al. 2001a). It is unclear how often this will happen, because—as we will see below—the fraction of meteorites with a complex exposure history is not well constrained and because it is also not well constrained how many meteorites with a large preatmospheric size go unnoticed as such. However, Bogard et al. (1995) note from a data survey that higher ^{36}Ar/^{38}Ar ratios are in general due to a higher contribution of primordial or atmospheric Ar rather than to a possible widespread presence of $^{36}Ar_n$, so the problem does not seem to be an ubiquitous one.

As Kr and Xe have more isotopes than Ar, an unambiguous determination of the neutron-capture component is easier in principle. Nevertheless, precise corrections for primordial or atmospheric Kr and Xe are often also difficult.

Isotopic abundances of cosmogenic noble gases

In order to deduce the cosmic-ray-produced fraction of a noble gas nuclide in a meteorite, it is commonly necessary to correct for other noble gas components, mostly trapped primordial gases or atmospheric contamination. To this end, the isotopic composition—or at least some crucial isotopic ratios—of the various components should be well constrained. Trapped components are discussed in previous chapters by Ott (2002) and Wieler (2002). Here we discuss the isotopic compositions of cosmogenic noble gases, which are summarized in Tables 3 and 4. As we have seen above, this composition will depend on the shielding and the chemical composition of a sample. Therefore, the values in Tables 3 and 4 should only serve as guidelines and the best values to be adopted may need to be evaluated from case to case.

Helium. Iron meteorites often contain essentially pure cosmogenic He, i.e., negligible radiogenic or atmospheric ^{4}He. The range of $(^4He/^3He)_{cos}$ given in Table 3 has been determined from the noble gas compilation by Schultz and Franke (2000), using relatively He-rich samples (^{3}He $> 200 \times 10^{-8}$ cc/g) of all iron meteorite classes. $(^4He/^3He)_{cos}$ correlates with the widely used shielding parameter ^{4}He/^{21}Ne, increasing with shielding from ~3 to ~4.5. However, this correlation is often disturbed in meteorites that suffered ^{3}H losses.

In most stony meteorites, ^{4}He is overwhelmingly radiogenic, such that $(^4He/^3He)_{cos}$ is difficult to measure directly (and of rather little practical concern). The two values given in Table 3 have both been derived from a suite of meteorites with low and presumably rather constant radiogenic ^{4}He. These are L chondrites which record a major collision on their parent body some 500 Myr ago that led to a

Table 3. Isotopic composition of cosmogenic He, Ne, and Ar.

	$^4He/^3He$	*Corresponding* $^4He/^{21}Ne$ *range*
iron meteorites	3.2-4.4	200-440
stony meteorites	5.2±0.3[1]	
	6.1±0.3[2]	
	$^{22}Ne/^{21}Ne$	*Corresponding* $^{20}Ne/^{21}Ne$ *range*
chondrites	1.05-1.25	0.88-0.98[a]
	$^{36}Ar/^{38}Ar$	*Corresponding* $^4He/^{21}Ne$ *range*
iron meteorites	0.60-0.665 (mean 0.63)	450-200
stony meteorites	~0.65	

1: Heymann (1967). **2**: Alexeev (1998); other values see text.
a: range somewhat uncertain, see text.

complete loss of the radiogenic ^{4}He accumulated up to that time (Swindle 2002b). Within their limits of uncertainty, the L chondrite values should also hold for other stony meteorite classes. This is also indicated by some stony meteorites, in particularly diogenites, which have measured ^{4}He/^{3}He ratios as low as ~5 due to very low U and Th concentrations (Welten et al. 1997).

Neon. We have seen above that $(^{22}Ne/^{21}Ne)_{cos}$ in stony meteorites is quite variable, which makes it useful as a shielding parameter. The range stated in Table 3 is for chondrites (see Fig. 6), and will be different for stony meteorites with rather different relative Mg, Al, and Si abundances. The differences can be estimated by means of Table 2. The $(^{20}Ne/^{21}Ne)_{cos}$ ratio in chondrites is difficult to evaluate because at least minor contributions of primordial or atmospheric ^{20}Ne are ubiquitous. Consideration of only ordinary chondrites of high exposure ages and high petrographic types 5 and 6 (i.e., little or no primordial Ne; Schultz and Franke 2000) suggests that $(^{20}Ne/^{21}Ne)_{cos}$ increases with increasing $(^{22}Ne/^{21}Ne)_{cos}$ (Table 3).

Argon. Iron meteorites again often allow direct measurement of the $(^{36}Ar/^{38}Ar)_{cos}$ ratio. Iron meteorites with relatively high $^{38}Ar_{cos}$ show an inverse correlation between ^{36}Ar/^{38}Ar and the shielding parameter ^{4}He/^{21}Ne (Table 3). $(^{36}Ar/^{38}Ar)_{cos}$ decreases by up to ~10% with higher shielding. The average value is ~0.63. Determining $(^{36}Ar/^{38}Ar)_{cos}$ in stony meteorites is again compromised by the common presence of primordial or atmospheric Ar and sometimes also by neutron-capture-produced ^{36}Ar. Yet, the lowest measured ^{36}Ar/^{38}Ar ratios in achondrites poor in primordial gases and with relatively high exposure ages are ~0.63, similar to the mean value of iron meteorites (Schultz and Franke 2000). More achondrite values cluster around ~0.65, however, which is a widely adopted $(^{36}Ar/^{38}Ar)_{cos}$ value for stony meteorites. It appears rather surprising that ^{36}Ar and ^{38}Ar are produced in almost equal proportion from the target elements Ca and Fe, respectively.

Krypton. The average isotopic composition of cosmogenic Kr in lunar soils and in chondrites is given in Table 4. These data are from compilations by Pepin et al. (1995) and Lavielle and Marti (1988). When correcting a measured Kr composition for a trapped component, the assumption is commonly made that the cosmic-ray-produced contribution on ^{86}Kr can be neglected, so that the measured ^{86}Kr can be assumed to be entirely trapped. Note that ^{80,82}Kr in different meteorites may contain variable contributions from

Table 4. Isotopic composition of cosmogenic Kr and Xe (relative to ^{83}Kr, ^{126}Xe ≡ 1)

	^{78}Kr	^{80}Kr	^{82}Kr	^{84}Kr	^{86}Kr			
average, lunar bulk soils[1]	0.20(2)	0.54(7)	0.72(5)	0.32(10)	≡0			
chondrites[2]	0.18(4)	0.60(8)	0.76(8)	0.67(15)	≡0			
	^{124}Xe	^{128}Xe	^{129}Xe	^{130}Xe	^{131}Xe	^{132}Xe	^{134}Xe	^{136}Xe
average, lunar bulk samples[1]	0.56(3)	1.48(6)	1.64(15)	0.95(7)	5.30(42)	0.77(20)	0.05(3)	≡0
Chondritic Ba/REE[3]	0.595(10)	1.52(10)		0.98(06)	3.77(16)	0.83(06)	0.044(15)	≡0
meteorites[4]	0.55(10)	1.40(15)	1.6(2)	1.0(2)	2.5(5)	1.0(2)	0	≡0

Uncertainties in ( ) given in units of the last digit. **1**: Pepin et al. 1995. **2**: Lavielle & Marti 1988, mean and standard deviation from 11 chondrites. **3**: Hohenberg et al. 1981, based on Angra dos Reis achondrite data. **4**: Kim & Marti 1992.

Table 5. Exposure age ranges and clusters of meteorite classes

Class	*Range (Myr)*	*Clusters (Ma)*	*Comments*
Chondrites			
H[1]	1-80	**7.6** & 33	all petrographic types
		7.0?	H5 a.m. falls only
		24	H6 only
L[2]	1-70	**40**	mainly L5 & L6
		28	mainly L5 & L6 & ^{40}Ar-poor
		15 & 5	^{40}Ar-poor
LL[3]	0.03-70	**15**	mainly LL5 & LL6 & ^{40}Ar-rich
		10?	LL6 only
		28?	mainly LL3
		40?	mainly LL4
EH & EL[4]	0.07-66	25? &	clusters need confirmation
		8? & 3.5?	
CO, CV, CK[5]	0.15-63	9?	CV, CK only
		29?	CO, CV, CK
CM & CI[6]	0.05-7	**0.22**	CM only (CI poor statistics)
R[7]	0.2-50		many ages between ~7-40 Ma
Other meteorites			
HED[a,8]	5-76	**21** & 38	H&E&D
		12?	Eucrites only?
		50?	diogenites only?
Aubrites[9]	~17-130	45-80??	cluster unclear (see text)
Lodranites-acapulcoites[10]	4-10		similar as 7 Ma peaks for H chondrites
Ureilites[11]	0.1-34		
Iron meteorites[b]	10-2300		
IVA[12]		255	^{36}Cl-^{36}Ar ages
		207	
IIIAB[13]		460	
Mesosiderites[14]	10-180		^{36}Cl-^{36}Ar ages
Lunar[15]	<0.01-8		hardly any source crater pairing
Martian[15]	0.7-20		4-9 events on Mars

Particularly conspicuous exposure age clusters in bold face, uncertain ones marked by ? **a**: Howardites-Eucrites-Diogenites. **b:** Ages of clusters of iron meteorites refer to ^{36}Cl age-scale (see text). In the ^{40}K-scale, the double peak at 255 & 207 Ma in group IVA corresponds to a single peak at 375 Ma, whereas the IIIAB peak at 460 Ma is shifted to 650 Ma (Voshage 1978, 1984). Oldest stated age of 2300 Myr (Deep Springs) refers to ^{40}K-scale.

References: **1**: Graf and Marti 1995; Graf et al. 2001. **2**: Marti and Graf 1992. **3**: Graf and Marti 1994; lowest age from ref. 4. **4**: Patzer and Schultz 2001. **5**: Scherer and Schultz 2000. **6**: Nishiizumi et al. 1993; Caffee and Nishiizumi 1997; K. Nishiizumi, pers. comm. 2000. **7**: Schultz and Weber 2001. **8**: Eugster and Michel 1995; Welten et al. 1997; Welten et al. 2001b. **9**: Eberhardt et al. 1965. **10**: Terribilini et al. 2000; **11**: Scherer et al. 1998. **12**: Lavielle et al. 2001. **13**: B. Lavielle 2001, pers. comm. **14**: Begemann et al. 1976. **15**: Wieler and Graf 2001. **16**: Nyquist et al. 2001.

neutron-capture on Br.

Xenon. The average isotopic composition of cosmogenic Xe in lunar samples and meteorites is also given in Table 4. The lunar data are again from Pepin et al. (1995).

Hohenberg et al. (1981) studied Xe in different mineral fractions of the Angra dos Reis achondrite and were able to derive separately the isotopic composition of the cosmogenic Xe produced by Ba and rare earth elements. The respective entry in Table 4 is for a chondritic value of $(La + Ce + Nd)/Ba = 0.52$. The value for meteorites given by Kim and Marti (1992) is modified from earlier data on chondrites and eucrites.

EXPOSURE AGE DISTRIBUTIONS OF METEORITES

Even though a single exposure age value may be equivocal, as we noted above, the impressive data base on exposure age distributions of individual meteorite classes available today provides crucial information on how meteorites are delivered to Earth. Exposure ages tell us mainly how long meteorites have been travelling as meter-sized objects in interplanetary space and peaks in exposure age histograms indicate common impact events that led to the ejection of many meteorites from a common parent body.

Most published exposure ages are based on noble gas analyses, which are compiled by Ludolf Schultz and coworkers at the Max Planck Institut für Kosmochemie in Mainz, Germany. In the year 2000, the compilation contained more than 6000 entries from more than 1500 meteorites (Schultz and Franke 2000). From these data, exposure ages for many hundreds of meteorites can be calculated. For meteorites with short exposure ages of a very few million years or less, radionuclide data are often also considered, in particular for carbonaceous chondrites of the classes CM and CI. A compilation of radionuclide data available up to the late 1980s is given by Nishiizumi (1987). Radionuclide-based exposure ages are reliable as long as the measured activity is sufficiently smaller than the saturation activity, so that the uncertainty of the latter is not a crucial factor in the calculation, i.e., for exposure ages up to perhaps two half-lives of the nuclide under consideration. For meteorite finds it must also be verified that an activity below saturation is not due to a long terrestrial age (see *Terrestrial ages* subsection).

A potential problem when studying exposure age distributions is a bias introduced by unrecognized "pairings," i.e., meteorite fragments from a common fall. This is a major concern especially for meteorites found in deserts. In Antarctica, sometimes dozens or hundreds of fragments recovered by organized searches belong to the same shower of a meteorite broken up in the atmosphere. For meteorites that are observed to fall, pairing is usually readily recognized, however. Exposure age histograms shown below are thus based either mainly on observed falls, or are corrected for pairing to the extent possible.

Figures 7-10 show exposure age distributions of most of the more common meteorite classes, and Table 5 summarizes the figures. We note the following first-order observations and conclusions:

(1) Most stony meteorites have nominal exposure ages ranging between a few and about 70 Myr. Apart from possible misassignments due to unrecognized complex exposures or grossly overestimated production rates, this interval thus indicates the range of times stony meteorites spend in space as small objects after ejection from their "immediate" parent body. Remarkable exceptions are the carbonacous chondrites of types CM and CI, which mostly show exposure ages below 1 Myr, and the aubrites, which on average have the longest exposure ages of all stony meteorites.

(2) Iron meteorites mostly have considerably longer exposure ages than stony meteorites, often amounting to several hundred million years. The iron meteorite Deep Springs has an exposure age of about 2.3 Gyr and hence has lived as a small object in interplanetary space for just about half the solar system lifetime. The highest exposure ages of stony-iron meteorites are in between the highest values of stony and iron meteorites, respectively. Because CI chondrites, and presumably also CMs, are more fragile than other stony meteorites, which in turn are more fragile than iron meteorites and probably also stony irons, it is certainly reasonable to conclude that mechanical strength influences the mean lifetime against collisional

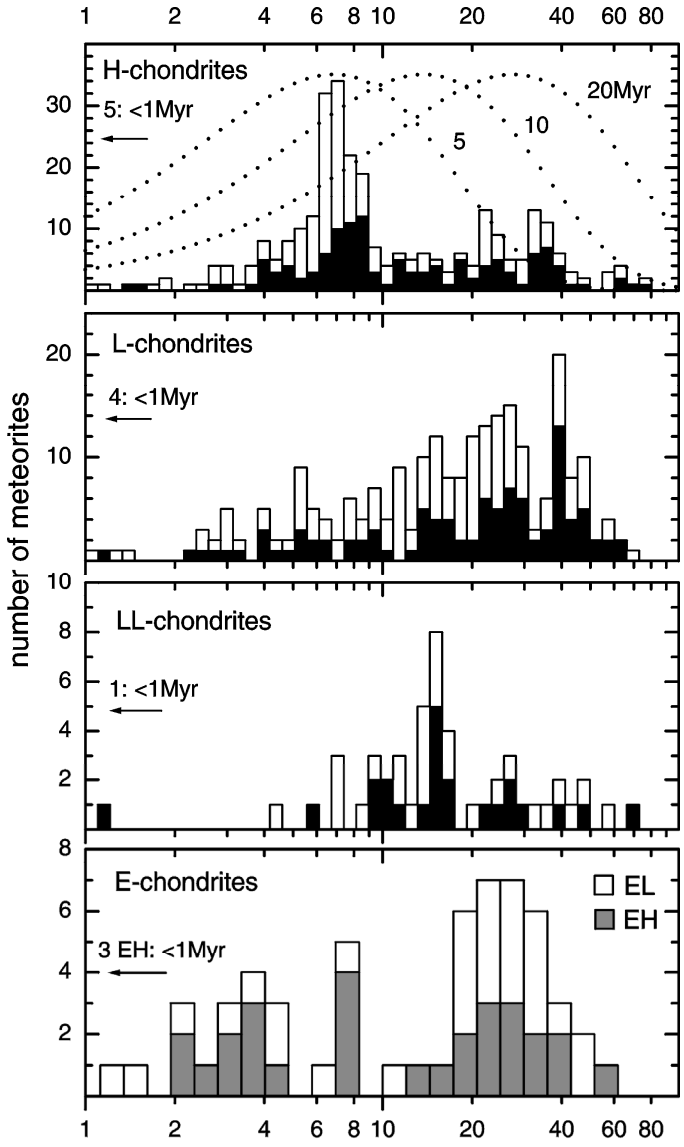

Figure 7. Exposure age distributions of ordinary chondrites (H, L, LL) and enstatite chondrites (EL, EH). The histograms for the ordinary chondrites are from the compilations by Marti and Graf (1992), Graf and Marti (1994, 1995), and updates (Th. Graf, pers. comm. 2001). The time resolution on the logarithmic abscissa scale is 10%, corresponding to the estimated accuracy of the highest quality data (class A of Graf and Marti, 1992; shown as filled bars in the top three panels). The E-chondrite histograms are from Patzer and Schultz (2001), with a time resolution of 20%. Some meteorites with nominal exposure ages < 1 Myr are off-scale and indicated by arrows. The dotted lines in the top panel represent expected exposure age distributions assuming continuous delivery and mean orbital lifetimes of 5, 10, and 20 Myr, respectively (Graf and Marti 1995).

destruction and thus is an important factor in determining meteorite exposure ages. Evidence for this is provided by the observation that chondrites with long exposure ages have lower $^{22}Ne/^{21}Ne$ ratios and hence larger masses than those with shorter ages (Loeken et al. 1992). On the other hand, this cannot be the whole story, as aubrites are more fragile than most other stony meteorite classes, and yet show unusually long exposure ages.

(3) Exposure age distributions of many, if not most, meteorite classes show one or more

clusters. In some cases, these clusters are very distinct, as the 7-Myr peak representing almost half of the H chondrites, the 15-Myr peak comprising a third of the LL chondrites and the 21-Myr peak that includes half of the HED meteorites. In other cases, peaks may require quite detailed data analysis to be recognized, as we will explain below, and sometimes it is unclear at all whether a couple of meteorites with similar exposure ages represent a statistically significant cluster. The most straightforward interpretation of these clusters is that each of them is the result of a—presumably very large—collision on a single immediate parent body. Each confirmed cluster thus indicates that a sizeable fraction of all meteorites of the respective class results from a few collisions. This is the view adopted in the following, although more complicated scenarios may be conceivable, such as producing exposure age clusters by a number of causally related collisions on different parent bodies of the same class within a short time.

We will next inspect exposure age distributions more closely, with the goal of obtaining additional information on the orbital and parent-body histories of meteorites. Later we will discuss this information in the context of dynamical models of meteorite delivery (see also Wieler and Graf 2001).

Undifferentiated meteorites

Exposure age distributions of ordinary chondrites have been investigated thorougly by Marti and Graf (1992) and Graf and Marti (1994, 1995). Slightly updated versions of their histograms are shown in Figure 7. The age scale is logarithmic with a bin-width of 10%, corresponding to the presumed uncertainty of the highest-quality data (Marti and Graf 1992).

H-chondrites. We consider first the ordinary chondrites of chemical class H in some detail (uppermost panel). As mentioned above, ~45% of all H-chondrites have exposure ages of ~7 Myr. This is the best studied exposure age peak (Graf and Marti 1995). It is rather broad, even for the highest quality data (filled histogram), which is a first indication that it might actually represent two events rather than one. A second cluster at 33 Myr comprises a further 10% of all H-chondrites. The probability that this second peak is just a statistical fluctuation in a quasi-continuous meteorite production process is estimated to be $< 0.5\%$ (Graf and Marti 1995). A third cluster at 24 Myr is not very conspicuous in Figure 7, in particular not in the highest quality data. However, this peak is rather prominent if the petrographic type H6 is considered separately, but completely absent in the other petrographic types (petrographic types H3-H6 indicate increasing thermal metamorphism; the respective histograms are shown in Graf and Marti 1995). Hence, three or four events account for almost two-thirds of all H chondrites or 20% of all stony meteorites that fall today. Note that the peaks at 24 and 33 Myr may well represent events of similar magnitude as the one or two events producing the larger 7-Myr peak, as older peaks will become less conspicuous due to the limited lifetime of meteorites discussed below.

That the 24-Myr peak appears only in a subset of all H chondrites is a good example of how detailed examinations may reveal collisional events that might go unnoticed otherwise. Unfortunately, most meteorite classes besides H and L chondrites are not numerous enough to allow such detailed assessments. The individual “7-Myr” peaks of types H4 and H5 are also displaced by roughly 1 Myr relative to each other, the H5s being older. Graf and Marti (1995) furthermore point out that H5 chondrites more often than other H chondrites have lost their cosmogenic tritium (and hence ^{3}He) due to heating during close passage by the Sun and that H5s do not show the excess of afternoon falls relative to morning falls that is typical for the other ordinary chondrite classes. These

observations indicate that a subgroup of the H5 chondrites experienced a special orbital evolution. It is possible that these are the meteorites formed in the older of the two presumed 7-Myr collisions, happening on a different parent body than that yielding the other 7-Myr H chondrites. This second collision and that at 33 Myr sampled several or all petrographic types of H chondrites, indicating that a structure according to petrographic type, perhaps layered with type 3 being near the top (Pellas and Fiéni 1988), is partly preserved on at least one of the immediate H chondrite parent bodies. The 24-Myr event may have happened on a part of this body dominated by H6 material or on a separate H6-rich immediate parent body.

In summary, three or four large collisions on one to four asteroids are responsible for two thirds of all H chondrites. It is often assumed that all H chondrites ultimately derive from a single asteroid, having broken up and partly reassembled early in solar system history (Keil et al. 1994). In this scenario, the parent bodies from which meteorites get delivered to Earth today would have been formed in these early or in later collisions. Cosmic ray exposure age studies cannot decide whether these immediate parent bodies—if more than one—indeed derive from a common ancestor.

Given that the majority of the H chondrites can be traced back to a very few collisions, it is reasonable to ask whether the remaining H chondrites which do not obviously belong to one of the major peaks were formed either by many smaller events as a quasi-continuous "background," or in a few other rather large collisions. It is also possible that the respective ages are wrong, and we will see in the *Complex Exposure Histories* section that this is probably indeed so for part, but not all, of the "non-peak" meteorites. Continuous background production has been modelled by Graf and Marti (1995). The dotted lines in the uppermost panel of Figure 7 show their expected exposure age distributions (not to scale) for constant production and three different mean lifetimes against either ejection from the solar system or collisions with a planet or the Sun (the apparent maxima of these curves at ~7-30 Myr are the result of the logarithmic scale on the abscissa). The observed distribution shows the same sharp drop-off at >60 Myr as the 10-Myr-lifetime curve and this model distribution may also be consistent with the small but discernible fraction of meteorites with exposure ages <4Myr. However, Graf and Marti (1995) point out that such young ages may often be flawed, so that many of the meteorites nominally younger than 4 Myr were actually created in one of the 7-Myr events. They concluded that the dotted lines do not represent a possible background population well, unless either minimum transfer times from the asteroid belt are several million years for all but possibly the fastest few meteorites, or the backgound was absent in the past few Myr. In conclusion, it is possible that many of the meteorites outside one of the large peaks are the result of a small number of additional rather large collisions (Graf and Marti 1995). We will further discuss this in the Ex*posure ages and dynamical models of meteorite delivery* subsection.

L and LL chondrites. The histograms of these two classes have many similarities with that of the H chondrites: one very conspicuous peak each (at 40 Myr for the L chondrites and 15 Myr for the LLs), no ages larger than some 70 Myr, and (for LLs) very few ages below 5 Myr. Note that the few L chondrites below 2 Myr are strongly shocked and possibly have an atypical collisional history (Graf and Marti 1994). Therefore the observation of a scarcity of very low-exposure ages to some extent also holds for L chondrites. As with the H chondrites, the L chondrites also have minor peaks (at 28, 15, and 5 Myr) that become prominent only in a subgroup, here the ^{40}Ar-poor L chondrites (Marti and Graf 1992). Many L chondrites show deficits in radiogenic ^{4}He and ^{40}Ar due to a major collision on their parent body roughly 500 Myr ago (Bogard 1995; Swindle 2002a). Interestingly, the LL chondrites show a minor peak at 28 Myr and possibly another one at 40 Myr, both at positions also occupied by L chondrite peaks (Graf and

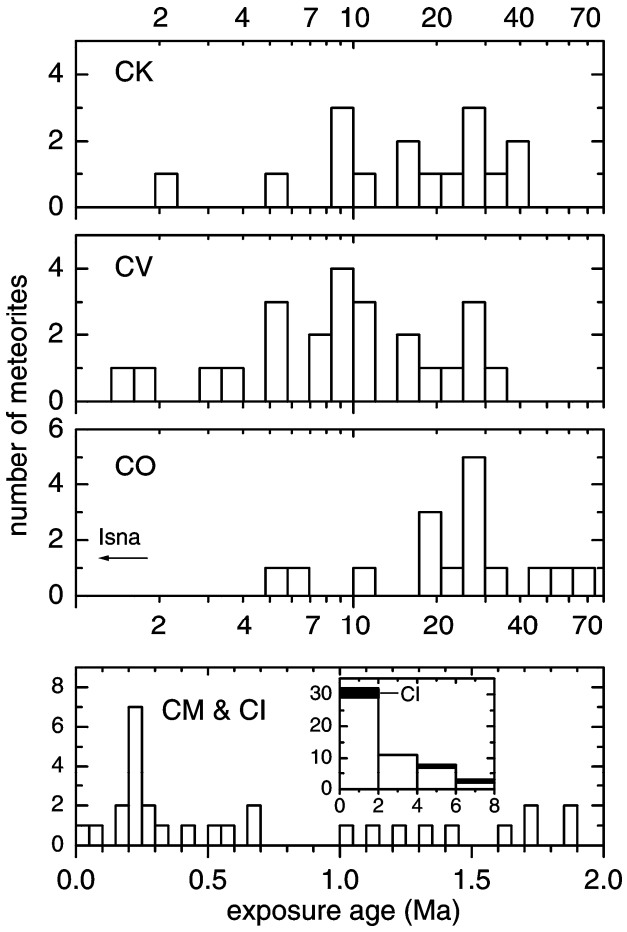

Figure 8. Exposure age distributions of carbonaceous chondrites. The top 3 panels (CK, CV, and CO chondrites) display data from Scherer and Schultz (2000) on a logarithmic time scale with 20% resolution. The bottom panel shows the histogram for the CM chondrites (including the few CI chondrite ages in the inset) according to Nishiizumi et al. (1993), Caffee and Nishiizumi (1997), and K. Nishiizumi (pers. comm., 2001). Note the widely different (linear) age scale in this panel.

Marti 1994). The LL chondrite Galim/a has an extraordinarily low-exposure age of 30,000 years only (Patzer and Schultz 2001).

Given these similarities in the exposure age distributions, the conclusions for L and LL chondrites are similar to those for the H chondrites: a very few collisions are responsible for a large fraction of the L and LL chondrites, and it is conceivable that most of the others were also created in a few additional events. If a quasi-continuous background exists, transfer times are mostly at least several million years.

Enstatite chondrites. A comprehensive study of exposure ages of enstatite chondrites by Patzer and Schultz (2001) indicates clusters at 3.5, 8, and 25 Myr (Fig. 7), although the authors caution that these peaks need to be confirmed, since both the age uncertainties for enstatite chondrites are larger than for ordinary chondrites, and the data base for E-chondrites still is comparatively small. Keil (1989) suggests that the two subgroups EH and EL derive from two different parent bodies. It is therefore instructive to compare the exposure age distributions of EH and EL chondrites, even though this is hampered by somewhat poor statistics. Patzer and Schultz (2001) note that the two distributions are not distinguishable from each other, which would be remarkable if the two classes derive from different parent bodies. Yet, the suspected peaks at 3.5 and 8 Myr do not show up in the EL chondrites. On the other hand, the most clear-cut peak at 25 Myr in the lowermost panel of Figure 7 is indeed seen in both types, EH and EL (although it is somewhat irritating that only very few of the 29 E chondrites compiled by Okazaki et al. 2000 have exposure ages around 25 Myr). We further note that, very similar to ordinary chondrites, ages >60 Myr are absent and quite few ages are below 2

Myr. A notable exception is the EH3 chondrite Galim/b, which seems to be an inclusion in the LL-chondritic polymict breccia Galim/a with an exposure age of only ~70,000 years (Patzer and Schultz 2001).

Rumuruti chondrites. Schultz and Weber (2001) report an age range of 0.2-50 Myr for 18 members of this class. Many ages fall between 7 and 40 Myr, but Schultz and Weber (2001) note that the remarkably low age of about 200,000 yr of the R chondrite Northwest Africa 053 demonstrates that short transfer times from the Asteroid belt are possible. The number of R chondrites is too low to expect clear-cut exposure age clusters.

Carbonaceous chondrites. Carbonaceous chondrites are in many respects the most primitive meteorites. The exposure age distributions of the various chemical classes reveal a clear dichotomy (Fig. 8). The CV, CO, and CK histograms essentially look very similar to those of the other stony meteorite classes, with most ages falling in the range of between a few Myr up to 40-60 Myr (Scherer and Schultz 2000). The very low age of only 0.15 Myr of the CO chondrite Isna is remarkable. On the other hand, the chemically most primitive classes CI and CM have strikingly low-exposure ages of less than 7 Myr, the majority of them falling between a mere 50 kyr and 2 Myr (Nishiizumi et al. 1993; Caffee and Nishiizumi 1997; Eugster et al. 1998a; K. Nishiizumi, pers. comm. 2001, see Wieler and Graf 2001). CV and CK chondrites possibly show a peak in their exposure age distribution at ~9 Myr and all three classes CV, CK, and CO may display a cluster at ~29 Myr (Scherer and Schultz 2000). If these common events could be verified, this would support the idea that these classes are closely linked to each other (Kallemeyn et al. 1991). CI meteorites are much too scarce to reveal any possible clustering, but CM chondrites show a very distinct peak at 0.2-0.25 Myr.

Why does the majority of CM and CI chondrites have such low-exposure ages in a range almost unoccupied by all other stony meteorite classes? We noted above that one reason may be the mechanical weakness of these meteorites and their parent bodies, which may strongly reduce their mean lifetime against collisional destruction. This would imply than CM (and CI?) chondrite meteoroids are abundantly produced. However, as also noted above, the high exposure ages of the fragile aubrites illustrate that other factors must be involved, such as mean transfer times and dynamical lifetimes, as discussed below. Perhaps the distinct 0.2- to 0.25-Myr peak is due to a collision on an immediate CM parent body with an orbit crossing that of the Earth (Caffee and Nishiizumi 1997). Besides the one distinct peak, the exposure ages of CM chondrites are distributed rather evenly, perhaps suggesting that a comparatively large fraction of them derives from relatively frequent smaller collisions.

Differentiated meteorites

HED meteorites. The Howardite-Eucrite-Diogenite (HED) clan is the largest class of achondrites. It is of particular importance here because it is believed that we know the parent body: the asteroid Vesta, or perhaps some of the smaller "Vestoids" thought to have been spalled off Vesta in a very large collision (Binzel and Xu 1993). The HED exposure age distribution (Fig. 9) is again strikingly similar to those of ordinary chondrites: all ages fall between 5-80 Myr, and distinct peaks emerge at 20-25 and 35-42 Myr (Eugster and Michel 1995; Welten et. al. 1997). Welten et al. (2001b) propose that there is an additional peak at ~50 Myr for the diogenites, although this is not resolved in Figure 9. Possibly as few as 5 or 6 events can explain most of the HED exposure ages (Eugster and Michel 1995; Welten et al. 1997). Based on this low number, Welten et al. (1997) and Bottke et al. (2000) favor Vesta rather than the Vestoids as the major HED source.

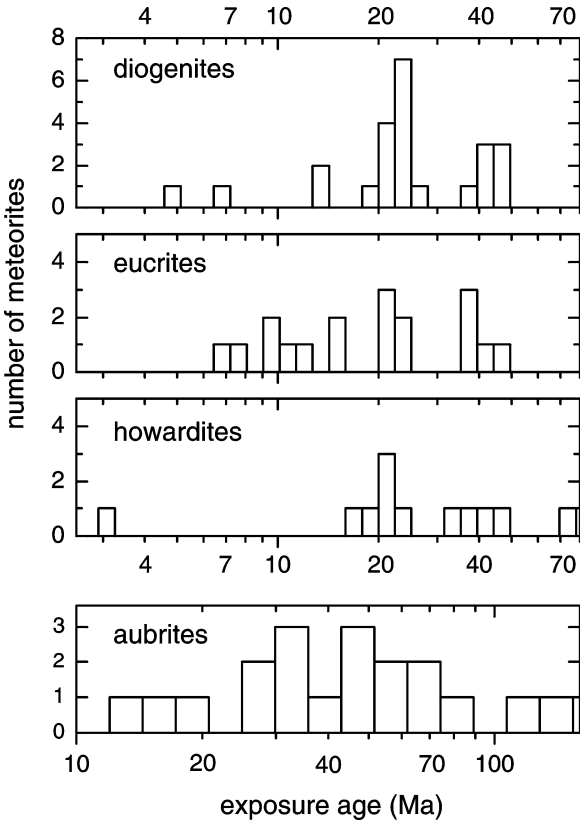

Figure 9. Exposure age distributions of HED meteorites (howardites, eucrites, diogenites) and aubrites or enstatite achondrites. The HED data are from the compilation by Welten et al. (1997), with only the (shielding corrected) ^{81}Kr-Kr ages being displayed for the eucrites. Included are 4 new diogenite ages from Welten et al. (2001b). In addition, the ~3 Myr age of the howardite Kapoeta has been added (Caffee and Nishiizumi 2001). For data sources of aubrites see text. Note the different abscissa scales between the lowermost panel and the others.

Aubrites (enstatite achondrites). This class is similar in many respects to enstatite chondrites, although the two classes are thought to derive from different parent bodies (Keil 1989). In the bottom panel of Figure 9, the exposure ages of aubrites are shown. These ages are more uncertain than those of chondrites, because production rate systematics have been less well studied for this rare class. The ages shown here rely on published cosmogenic Ne data (Schultz and Franke 2000) and the production model by Leya et al. (2000a), or, in a few cases, on ^{81}Kr-Kr analyses (Miura et al. 2000). In addition, we include ages given for eight aubrites from Antarctica by Lorenzetti et al. (2001). In the first systematic study of the cosmic ray record of aubrites, Eberhardt et al. (1965) already noted that aubrites have unusually long exposure ages among stony meteorites. This has become even more accentuated as the production rates we adopt here are lower than those used by Eberhardt and coworkers. Note on the other hand that the exposure age of the Norton County aubrite of 240-280 Myr reported by Begemann et al. (1957) has later been revised downwards and is shown here as only 130 Myr. Yet, it is quite remarkable that this meteorite with the first ever published cosmic ray exposure age still holds the record among stones, within uncertainties together with Mayo Belwa, another aubrite (Lorenzetti et al. 2001). Eberhardt et al. (1965) noted a cluster at 40-50 Myr, but uncertainties in production rates are too large to confirm this cluster in Figure 9 (at roughly 50-60 Myr with present-day production rates). Nevertheless, exposure ages of aubrites clearly are higher than those of most enstatite chondrites, consistent with the conclusion that aubrites derive from a separate parent body. The long interplanetary journeys of the fragile aubrites also indicate a distinctly different orbital evolution compared to other meteorite classes, resulting in longer survival times against ejection from the solar system or collision with a planet, as already pointed out by Eberhardt and coworkers.

Acapulcoites and lodranites. These meteorite classes, also called *primitive*

achondrites, are believed to derive from the same parent body and are residues from partial melting of chondritic precursors (McCoy et al. 1997). Exposure ages of both classes show a remarkably tight clustering between 4 and 10 Myr, in the same range as the prominent 7 Myr cluster of the H chondrites (Weigel et al. 1999; Terribilini et al. 2000a; Ma et al. 2001). Terribilini et al. conclude that this may be due to one impact (with subsequent secondary break-ups of a larger meteoroid) or several impacts closely spaced in time. They point out that the coincidence of exposure age clusters of acapulcoites/lodranites and H chondrites might suggest an enhanced collisional activity in the asteroid belt some 7 Myr ago.

Ureilites. Goodrich (1992) and Scherer et al. (1998) compiled exposure ages of ureilites. Values range between 0.1 and 34 Myr. Again, the majority of the ureilites, i.e., >70% of the 22 meteorites compiled by Scherer et al. (1998), have ages above 3 Myr. No exposure age clusters are observed. However, since many ureilites contain relatively large amounts of primordial Ne, a shielding correction via $^{22}Ne/^{21}Ne$ is often not possible. Therefore, exposure ages of ureilites often have a quite high uncertainty, and so clusters, even if present, might be less easily recognized than in other meteorite classes. Mean activities of ^{10}Be and ^{26}Al in ureilites are ~20% lower than expected, indicating that many ureilites had a small preatmospheric size (Aylmer et al. 1990).

Iron meteorites and stony-irons. Reliable exposure ages for iron meteorites are often even more difficult to obtain than for stony meteorites, because quite a few iron meteorites had preatmospheric sizes of one to several meters, so that large production rate variations due to variable shielding are common. As a somewhat extreme example, ^{3}He concentrations in fragments of the R ~15 m Canyon Diablo meteorite vary by a factor of 10,000 (Heymann et al. 1966), and even in the 13 most gas-rich samples analyzed by these authors, He, Ne, and Ar concentrations varied by ~20 to 35 times. Reliable corrections for production rates over a wide range of shielding are therefore a prerequisite in exposure age studies of iron meteorites. Considerable efforts are being spent to achieve this, because iron meteorites often have much higher exposure ages than stony meteorites and therefore are particularly important for studying possible long term variations of the flux of the galactic cosmic radiation. Three main methods are He-Ne-Ar, ^{40}K-^{41}K, and ^{36}Cl-^{36}Ar. The relationship between noble gas production rates in iron meteorites and shielding parameters such as $^{4}He/^{21}Ne$ has been described by Signer and Nier (1960, 1962) using a semiempirical model. The ^{40}K-^{41}K method, involving the very long-lived radionuclide ^{40}K (half-life 1.25 Gyr) has been developed by H. Voshage (Voshage 1978 1984, and references therein) and the ^{36}Cl-^{36}Ar method has recently systematically been applied to iron meteorites by Lavielle et al. (1999a, 2001). These latter studies are also discussed in section *The Cosmic Ray Flux in Time*.

Figure 10 shows the exposure age distribution of iron meteorites. Ages >200 Myr are based on the ^{40}K-^{41}K method (Voshage 1978), while younger ages are based on ^{38}Ar (Lavielle et al. 1985), because few K-ages exist for the age range 0-200 Myr. The Figure may thus well be biased somewhat due to sample selection, possibly underestimating the fraction of iron meteorites with relatively low-exposure ages. The abscissa may also be compromised by a possible GCR intensity change as discussed in section *The Cosmic Ray Flux in Time*. Nevertheless, it is clear that the majority of iron meteorites has exposure ages exceeding the highest known age of a stony meteorite of some 130 Myr or so. Two clusters of exposure ages have been recognized for a long time, indicating major collisions on the IIIAB and IVA iron meteorite parent bodies about 650 Myr and 375 Myr ago, respectively, using the ^{40}K-age scale (Voshage 1978; Lavielle et al. 1985). Lavielle et al. (2001) proposed that the 375 Myr peak actually represents two events at 255 and 207 Myr ago in the ^{36}Cl-scale, whereas the 650-Myr peak corresponds to an event at 460 Myr in this scale (Lavielle 2001, pers. comm). In contrast to other iron

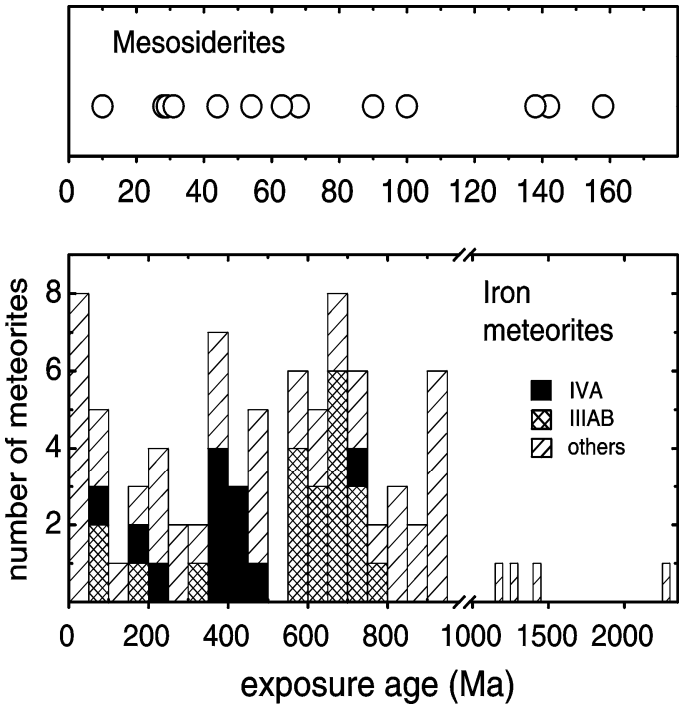

Figure 10. Exposure age distributions of iron meteorites and mesosiderite stony-irons. Iron meteorite data > 200 Myr were obtained by the ^{40}K-^{41}K method (Voshage 1978), ages < 200 Myr are based on ^{38}Ar (Lavielle et al. 1985). Iron meteorite groups IVA and IIIAB show exposure age clusters around 375 and 650 Myr (^{40}K-scale) and are shown separately. The 375 Myr cluster appears to be composed of two independent peaks not shown here (at 207 and 255 Myr in the ^{36}Cl-scale, see text). Mesosiderite ages (^{36}Cl-^{36}Ar) are from Albrecht et al. (2000), as updated from Begemann et al. (1976). Note the widely different abscissa scales of the two panels.

meteorites, the two classes IIA and IIE show exposure age ranges not unlike those of stony meteorites. Ages of IIA and IIE irons may be as low as a few Myr (Olsen et al. 1994), with the most reliable among the lowest values being around 10 Myr (e.g., Rafrüti: Terribilini et al. 2000b; Kodaikanal, Braunau, and Watson: Lavielle 2001, pers. comm.).

A study by Begemann et al. (1976), updated in Albrecht et al. (2000), determined ^{36}Cl-^{36}Ar ages of 16 stony-iron meteorites, mostly mesosiderites (Fig. 10). The values fall between ~10-180 Myr (10-160 Myr for mesosiderites alone), with about a third of the values being larger than 100 Myr. The age range for stony-irons is thus broadly in between those of stones and most irons. Welten et al. (2001c) note a hint for an exposure age cluster around 60-70 Myr.

The comparatively very old exposure ages of iron meteorites, and perhaps also the rather high ages of stony irons, are probably partly the result of their mechanical strength and hence long survival times against collisional destructions. Long collisional lifetimes could also explain why iron meteorites probably derive from considerably more parent bodies than stony meteorites. Petrographic and chemical evidence suggests that there are 90 or so different original iron meteorite parents (Wasson 1995), and a large number of them are sampled only by relatively small meteorites (Wasson 1990).

Lunar and Martian meteorites. At the time of this writing, our collections contain about 20 individual meteorites (corrected for pairings) from the Moon and 18 from Mars. A list of the Martian meteorites is given by Swindle (2002b), who also briefly discusses their cosmic ray record. Exposure ages of Martian meteorites are also compiled and

discussed in detail by Nyquist et al. (2001). Cosmogenic noble gases and radionuclides are a major tool for deciding whether different meteorite specimens, e.g., found in a desert nearby to each other, belong to the same fall or whether different meteorites from any find location were ejected by the same event (source crater pairing).

Quite as expected, most meteorites from the nearby Moon have had considerably shorter transit times than the meteorites from the asteroid belt discussed so far. Most exposure ages of lunar meteorites are below 1 Myr, and many even below 0.1 Myr. Very remarkable is the short transit time of Dhofar 026 of at most 4 Kyr (Nishiizumi and Caffee 2001). The highest age found so far is ~8 Myr (Polnau and Eugster 1998; Nishiizumi et al. 1999). Very few, if any, lunar meteorite falls are source crater paired (Warren 1994). Essentially all lunar meteorites have a complex exposure history, i.e. they also contain cosmogenic nuclides acquired on the Moon (e.g., Warren 1994; Polnau and Eugster 1998). This means that most lunar meteorites were ejected in relatively minor cratering events from within the uppermost very few meters of the lunar surface, where they had previously spent up to several hundred million years. Nishiizumi et al. (1999) note a correlation between the depth of ejection and the transit time to Earth, with meteorites from smaller events arriving earlier.

Martian meteorites had travelled for considerably longer than lunar meteorites, with transit times of between 0.7 and 20 Myr (Nyquist et al. 2001). Unlike for lunar meteorites, source crater pairing is common for Martian meteorites. The number of individual ejection events on Mars needed to account for the available meteorites is controversial, however (see also Swindle 2002b). Based on crystallisation ages, four to five impacts were proposed by Nyquist et al. (1998) (see also Nyquist et al. 2001). On the other hand, exposure ages suggest 7-9 events (Nyquist et al. 2001, Nishiizumi et al. 2000; K. Nishiizumi, pers. comm. 2000). Nyquist et al. (2001) discuss scenarios involving secondary collisions to reconcile the two lines of evidence. Since, unlike lunar meteorites, none of the Martian meteorites show signs of a complex exposure (Warren 1994; Nyquist et al 2001; however see also Hidaka et al. 2001), the bodies originally launched from Mars would have to have been quite large. The apparently single-stage exposure history also indicates that all Martian meteorites were launched from at least a few meters below the Martian surface (Warren 1994). A caveat to this conclusion is that a parent body exposure stage is more difficult to detect in meteorites having had a longer subsequent exposure during their transit to Earth. However, Martian meteorites on Earth are usually considerably larger than their lunar counterparts and hence probably also had a larger preatmospheric size, which also suggests that they stem from larger events than lunar meteorites. This is indeed expected given the different escape velocities from the two planets.

Micrometeorites and interplanetary dust particles (IDPs). The noble gas record in micrometeorites and IDPs is discussed by Wieler (2002). Cosmic ray exposure ages of micrometeorites from Greenland (Olinger et al. 1990) and of deep-sea spherules (Raisbeck and Yiou 1989) are between < 0.5 and 26 Myr, suggesting a cometary origin of most of these particles (Raisbeck and Yiou 1989). Cosmic ray exposure ages of IDPs are uncertain. Pepin et al. (2001) report large ^{3}He excesses in some IDPs which, if cosmic-ray-produced, would imply GCR ages of up to more than one Gyr, much larger than orbital lifetimes of small particles. The authors consider that this might be due to very long exposures in the regoliths of Kuiper Belt comets, but they also discuss the possibility that the excess ^{3}He is primordial (see Wieler 2002).

Exposure ages and dynamical models of meteorite delivery

Here we discuss constraints imposed by the observed distributions of exposure ages on ideas and models of how meteorites get delivered to Earth from the asteroid belt, the

Moon and Mars (see also Wieler and Graf 2001).

Stony meteorites from the asteroid belt. It has been known for a long time that ~15% of all meteorites falling today were produced in one—or more probably two—collisions manifested in the prominent 7 Myr peak in the exposure age histogram of the H chondrites. It has often been thought, however, that this was an exceptional event and that a quasi continuous production of meteorites in many smaller events is the rule. We have seen above that to some extent this discussion goes on today, as it remains open whether most of the meteorites not obviously belonging to a major peak in an exposure age distribution should be assigned to the "background" or to one of a few additional events, and how many of even these meteorites should be shifted to one of the large peaks. Furthermore, for all but the most common meteorite classes, even the quite impressive data base available today still often does not allow an unambiguous recognition of peaks. Nevertheless, exposure age peaks are identified or suspected in the histograms of many classes, which allows us to reiterate a conclusion already made by Anders (1964): a large part of the meteorites were produced in a few distinct major collisions. The quantification of this statement is somewhat difficult, but we note that more than 50% of all H chondrites derive from a few events, whereas small iron meteorites appear to be due mostly to a quasi continuous production.

It also has long since been recognized that orbital resonances with planets are a major factor determining the delivery of meteorites from the asteroid belt (Wetherill and Williams 1979; Wisdom 1983; Gladman et al. 1997; Farinella et al. 2001). Until recently, a common assumption was that the velocity of meteorites ejected from their parent asteroids needs to be sufficiently high to place them into a resonance, e.g., the 3:1 Kirkwood gap in the main asteroid belt, where an object orbits three times around the Sun in the time it takes Jupiter to complete one orbit. This has led to the hypothesis that only large collisions on parent bodies close to a resonance could produce large numbers of meteorites on Earth. This would qualitatively explain the distinct peaks in exposure age histograms, but it might be difficult to account for the observed flux of meteorites with the limited number of viable parent bodies (see discussion by G.W. Wetherill in Greenberg and Nolan 1989). Recent dynamical models now indicate that objects placed into a so-called chaotic zone in a resonance will have a much shorter dynamical lifetime than has previously been thought. Within a very few million years they will either collide with the Sun or be ejected from the solar system (Gladman et al. 1997). As these times are considerably less than typical exposure ages of almost all meteorite classes, in this scenario most meteorites need to spend most of their lifetime as meter-sized objects in the main belt, slowly drifting into a resonance (Morbidelli and Gladman 1998). It has recently been realized that the asymmetric radiation of thermal energy, the so-called Yarkovsky effect, can provide enough momentum to allow meter-sized objects to drift into a resonance on timescales comparable with meteorite exposure ages (e.g., Bottke et al. 2000). The Yarkovsky effect appears to be able to explain also the paucity of meteorites with exposure ages less than a few million years (Bottke et al. 2000). If so, asteroids throughout large parts of the main belt may be potential meteorite parent bodies. This, however, is only compatible with the marked peaks in the exposure age distributions, if a very few ones among these many potential parent asteroids contribute a major part of all meteorites. These selected bodies presumably should be among the largest asteroids. Wieler and Graf (2001) discuss some evidence that this might indeed be the case. On the other hand, the original H chondrite parent body or parent bodies, responsible for a large fraction of all meteorites today, were rather small, with a radius of only about 100 km (Pellas and Fiéni 1988). Bottke et al. (2000) also discuss this problem. Clearly, exposure age distributions with improved temporal resolution will be needed to further rule on the importance of the Yarkovsky effect as meteorite delivery mechanism.

Even though meteorites may be brought to Earth quickly from within a resonance in the main belt, it is not clear whether the 0.2-Myr peak of the CM chondrites can be explained this way. This would require a very large collision on a CM parent body in a position where the time needed to drift into a resonance would be extremely short and from which we would see today perhaps just some forerunners. It appears more likely that the 0.2 Myr CM chondrites are the products of a collision on a parent body already on an orbit crossing that of the Earth (Caffee and Nishiizumi 1997).

Iron meteorites. Meter-sized iron meteorites have a slower Yarkovsky drift rate than stones of the same size (Farinella et al. 2001), which is in qualitative agreement with the much older exposure ages of iron meteorites (see also Bottke et al. 2000; Morbidelli and Gladman 1998). The old ages lead to the expectation that many more collisions are recorded in the iron meteorite histograms compared to those of stony meteorites, consistent with the rareness of peaks in the former. The comparatively large number of iron meteorite parent bodies can be explained if iron meteorites are able to drift into a resonance from even larger portions of the belt than stones, because of their longer collisional lifetimes due to their mechanical strength. Wasson (1990) proposed that small iron meteorites move faster through the belt than large ones due to their higher ejection velocity, which would account for the high number of parent bodies sampled by small iron meteorites.

Lunar and Martian meteorites. Gladman et al. (1996) calculate that most lunar meteorites that end up on Earth do so within several 10^4 years. Fragments escaping this fate will reach orbits outside the Earth's immediate influence after about a million years. The calculations are thus essentially in agreement with the observations. Gladman (1997) calculates transfer times from Mars in agreement with the observed exposure ages for material ejected just slightly above escape velocity. Martian meteorites travel much longer than lunar ones simply because the orbits of Martian ejecta will not cross Earth's orbit initially. Given the closeness of the Moon, it appears astonishing that we do not have many more lunar than Martian meteorites. Gladman (1997) notes, however, that the higher fraction of escaped lunar meteorites that end up on Earth and the higher number of fragments per impact on the Moon may be largely offset by higher cratering rates on Mars and the fact that many Martian meteorites are source-crater-paired. It is thus not quite clear whether or not the similar numbers of lunar and Martian meteorites actually constitutes a puzzle. If it does so, this may be explained by mechanical properties of the two planetary surfaces. The low porosities of lunar meteorites suggest that compaction of loose regolith and simultaneous ejection may not work so that only the small fraction of already coherent rocks on the lunar surface may have a chance to end up as meteorites (Warren 2001).

COMPLEX EXPOSURE HISTORIES

The term *complex exposure* is commonly used to denote a situation where an entire meteorite acquired part of its cosmogenic nuclides detectable today in a larger body than the one immediately prior to atmospheric entry. A complex exposure history thus indicates a break-up of a precursor meteoroid or an ejection of a meteoroid from a near-surface location of a parent asteroid or planet. In the first case we talk about two different so-called 4π exposure stages, in that during both stages each sample saw cosmic rays from all directions in space, while in the second case a 2π irradiation is followed by the 4π exposure. It may also occur, however, that only certain parts of a meteorite (e.g., clasts or individual mineral grains) show excesses of cosmogenic nuclides relative to other fractions of the meteorite. This is commonly called *pre-compaction* exposure, and the precompaction stage may have occurred early in solar system history or later in a dust and gravel layer on the parent body surface, the *regolith*.

Thus, meteorites with a complex exposure history may help us to constrain collisional dynamics in the asteroid belt, the dynamics of asteroidal regoliths, and perhaps the energetic particle environment in the early solar system. On the other hand, we mentioned above that complex exposure histories often hinder our efforts to determine exposure age distributions.

Sometimes, a complex exposure history is quite easily recognized, for example if cosmogenic noble gases indicate an exposure during several ten million years in an average-sized meteorite, whereas the ^{10}Be activity is lower than the saturation value of medium-sized meteorites. Often, however, analyses of many different nuclides in different samples, if possible from well defined positions relative to each other, are required to unambiguously decide whether a meteorite had a simple or complex history. Nuclides such as ^{60}Co with its steeply rising production rate with preatmospheric depth (e.g., Heusser et al. 1996; see Fig. 1) or nuclear tracks with their steeply declining production rate with preatmospheric depth (Bhattacharya et al. 1973) are particularly useful but such data are rarely available (and ^{60}Co has decayed completely a few decades after the fall of a meteorite). It should thus not come as a surprise that only for few meteorites a complex exposure history has been unambiguously documented or at least found to be very likely. Vogt et al. (1993) and Herzog et al. (1997) list just 15 stony meteorites with a probable or certain complex history. It is even more difficult to exclude a complex exposure history (a prominent example is Knyahinya, where from numerous analyses a single stage lasting ~40 Myr has been deduced; Graf et al. 1990b). Therefore, the fraction of meteorites with a complex history cannot be estimated with confidence. Wieler and Graf (2001) guess that it could be around 30% for stony meteorites. Similarly, Lavielle et al. (1985, 2000) note that about one-fourth of all iron meteorites show indications of a complex history.

Some meteorites with a well documented complex history are Jilin, Bur Gheluai, Tsarev, Torino, Gold Basin and QUE93021 (Begemann, et al. 1996; Vogt et al. 1993; Wieler et al. 1996; Welten et al. 2001d,e). The second stages lasted on the order of 1-15 Myr and the first stages sometimes up to a hundred or a few hundred million years. The size of the first stage body is often unconstrained, but very long first stages seem to require an asteroidal parent body. Meteorites with nominally short exposure ages appear to often show a discernible complex history (Herzog et al. 1997; Merchel et al. 1999). This is not too surprising, because a first stage contribution is easier to detect if the subsequent second stage lasted only briefly. In these examples, first stages typically lasted on the order of 10 Myr, second stages only around a few hundred thousand years. This does not mean, however, that very low 4π exposure ages are more common than it may appear from the exposure age histograms, because the first stage may already have occurred in a meteorite-sized body rather than on a parent asteroid. This is illustrated by the H-chondrite Jilin, which is a good example of how complex histories smear out peaks in exposure age histograms. Jilin was probably ejected in one of the 7-Myr events and broken up in a second collision 0.3 to 0-6 Myr ago, whereas calculated single stage ages are between 1-5 Myr only, depending on the sample analysed (Begemann et al. 1996; Heusser et al. 1996). We mentioned above that a large part of the few H chondrites with <7-Myr nominal ages may have left their parent body in one of the 7-Myr events. On the other hand, it is worth repeating here that the mere existence of peaks in exposure age histograms is compelling evidence that the single stage assumption yields correct ages for a large part of all meteorites. Hence, while unrecognized complex exposures do compromise exposure age histograms to some extent, this even strengthens the

conclusion that a large fraction of all meteorites is produced in a very limited number of collisions in the asteroid belt.

Pre-compaction exposures. When parts of a meteorite show excesses of cosmogenic nuclides with respect to other parts of the same meteorite, and when these excesses cannot be explained by higher production rates due to higher concentrations of major target elements or favourable shielding, then the excesses must have been acquired before the various constituents of the meteorite were assembled as they are observed today. Such pre-compaction exposures are often recognized in so-called gas-rich meteorites, which contain noble gases implanted by the solar wind and represent compacted dust and pebbles from the surface regolith of an asteroid. Cosmogenic noble gas excesses have also been reported in single mineral grains or single chondrules from meteorites with no obvious signs of a parent-body-regolith exposure. These excesses may indicate an irradiation by an intense Sun in the early solar system. It might also be feasible to determine the lifetime of presolar grains before they were incorporated into meteorite parent bodies. These three topics are discussed in the following.

Gas-rich meteorites usually are a mixture of compacted solar-gas-bearing dust (matrix) and solar-gas-free cm-sized pebbles (inclusions). Often the matrix is darker than the inclusions. In many meteorites studied in detail, some of the inclusions contain excesses of cosmogenic noble gases, corresponding to 2π exposures on the order of millions to tens of millions of years (e.g., Wieler et al. 1989b and references therein; Pun et al. 1998). Commonly this is interpreted as the time a pebble spent near the surface of its parent body regolith, or, more exactly, as the differences of the regolith exposure durations of different pebbles. Compared with exposure ages in the lunar regolith of a few hundred million years, meteoritic regoliths are thus less mature, i.e., they had less time to evolve under the influence of (micro)meteorite bombardment and solar and galactic particle irradiation. Some of the inclusions are xenolithic and hence must ultimately derive from another parent body than their host meteorite (e.g., St. Mesmin Schultz and Signer 1977; Fayetteville: Wieler et al. 1989b; Kapoeta: Pedroni 1989; Pun et al. 1998). The respective excesses may therefore at least partly have been acquired on the grandparent body or perhaps while the future xenoliths were on their way to their foster parent bodies. Caffee and Nishiizumi (2001) studied ^{10}Be in clasts of the gas-rich howardite Kapoeta known to contain excess ^{21}Ne. They did not find ^{10}Be concentrations above those expected to have been acquired during ~3 Myr of meteoroid exposure, which indicates that the parent body exposure that produced the ^{21}Ne excesses had not occurred immediately prior to the ejection of the Kapoeta meteoroid. Regolith compaction and meteorite ejection therefore did not happen at the same time, at least not in the case of Kapoeta.

Matrix samples of gas-rich meteorites often also contain excess cosmogenic noble gases (Wieler et al. 1989a, Pedroni 1989; Assonov et al. 1996; Bogard et al. 2001), corresponding again to parent body exposure ages of a few 10^6 to a few 10^7 years. In some meteorites, the concentrations of solar and cosmogenic noble gases correlate well with each other, as may be expected (Wieler et al. 1989a; Assonov et al. 1996).

The group led by Charles Hohenberg in St. Louis has extensively studied cosmogenic ^{21}Ne in single mineral grains or batches of grains from several meteorites (Caffee et al. 1983, 1987; Hohenberg et al. 1990; Woolum and Hohenberg 1993). The grains were selected according to the presence or absence of solar-flare tracks, acquired while a grain was within the top few mm of the parent body surface. The track-rich grains almost all contained large excesses of cosmogenic Ne, whereas the track-poor grains did not. The excesses correspond to parent body exposure times to galactic cosmic rays of several 10^7 to several 10^8 years. Because this appeared too long, it was proposed that the

cosmogenic Ne in the track-rich grains was due to an irradiation with a high flux of energetic particles from the early Sun, which was far more active then than today (Caffee et al. 1983, 1987). In these early studies, mostly gas-rich meteorites were studied, which led Wieler et al. (1989a, 2000a) to propose the alternative explanation that the correlation of solar flare tracks with cosmogenic Ne excesses was produced by mixing of parcels of mature parent body regolith, which had been in the top meter or so for tens of millions of years, with less mature regolith. In this view, the Ne excesses are due to GCR production in the parent body regolith.

Whereas the long parent-body GCR irradiation scenario appears quite straightforward to explain the single grain data from gas-rich meteorites, even larger ^{21}Ne excesses were subsequently found in individual track-rich olivine grains from several carbonaceous chondrites of type CM (Hohenberg et al. 1990). The implied regolith GCR exposure ages of at least ~150 Myr, but more probably ~300 Myr, appear unreasonably long (Woolum and Hohenberg 1993). Therefore, the CM chondrite data are the most promising candidates for revealing evidence of an early active Sun. On the other hand, the solar flare track densities in CMs might be expected to be higher than observed if the cosmogenic Ne excesses were due to solar cosmic rays (Woolum and Hohenberg 1993; Wieler et al. 2000a).

Polnau et al. (1999, 2001) reported for several meteorites systematically higher concentrations of cosmogenic noble gases in chondrules than in matrix samples of the same meteorite. The excesses would correspond to 4π ages on the order of 0.1-3 Myr. The authors exclude the possibility that this is due to preferential gas loss from the fine-grained matrix, or to systematic errors in the corrections for variable target element chemistry, and conclude that the chondrules contain noble gases from a precompaction exposure. Only one of the meteorites studied contains solar noble gases (Polnau et al. 1999) and is therefore expected to show effects of pre-exposure in the parent body regolith. Polnau et al. (2001) therefore suggest that the chondrules in the other meteorites may have experienced exposure in a very high flux of solar energetic particles in the early solar system. This conclusion deserves further verification, especially by meteorites with very short exposure ages.

Lewis et al. (1994) calculated the pre-compaction ages of presolar SiC grains in primitive meteorites based on their concentrations of cosmogenic ^{21}Ne (after correcting for the ^{21}Ne produced in the recent irradiation of the host meteoroids). These ages are important for understanding the provenance of the grains and their history before incorporation into larger solid bodies in the early solar system (see Ott and Begemann 2000). The presolar ages derived by Lewis et al. (1994) of between ~10 and ~130 Myr were surprisingly low, with larger grains showing higher ages. Later, Ott and Begemann (2000) invalidated these ages when they showed that the loss of cosmogenic ^{21}Ne from micron-sized SiC grains due to recoil is much larger than was assumed by Lewis et al. (1994). In fact, the recoil loss rates of ^{21}Ne are so large as to inhibit a meaningful correction, except perhaps for the largest grains. Cosmogenic ^{126}Xe may be more promising (Ott and Begemann 2000; Ott et al. 2001), because of its considerably lower recoil range compared to ^{21}Ne.

Space erosion. It is conceivable that meteoroids change their shape not only by a macroscopic collision but by continuous erosion by micrometeorites in space. This space erosion has occasionally been invoked to explain discrepant exposure ages based on various nuclide systems. However, no generally accepted space erosion rates appear to have been derived and space erosion is not routinely taken into account when deducing exposure ages of meteorites. Voshage (1984) estimated space erosion rates on the order of 0.1 mm/Myr for iron meteorites by comparing the minimum depths of iron meteorite

samples with variable exposure ages, but he cautioned that this might not be a well constrained estimate, as simulation experiments yielded about 5 times lower values (Schaeffer et al. 1981). Space erosion rates on the lunar surface are usually assumed to be on the order of ~1 mm/Myr (e.g., Kohl et al. 1978). If these values apply to stony meteorites also, detectable effects would hardly be expected or would be limited to meteorites with exposure ages of at least several 10^7 Myr. Schaeffer et al. (1981) deduced a value of 0.65 mm/Myr for stony meteorites. However, Welten et al. (2001b) observed systematic differences between ^{10}Be/^{21}Ne and ^{21}Ne ages for diogenites with high exposure ages, whereas both methods yield consistent ages for younger diogenites. This might be explained by a space erosion rate of ~5 mm/Myr. Welten and coworkers caution that their observation might instead indicate a combination of (microscopic) space erosion and repeated chipping-off of larger fragments. On the other hand, if meteorites indeed spend most of their lifetime as meter-sized objects in the main asteroid belt as is indicated by modern dynamical models (see *Exposure ages and dynamical models of meteorite delivery* subsection), space erosion rates might be larger than commonly assumed due to a higher flux of micrometeorites. It therefore appears advisable to reconsider the issue of space erosion. Perhaps, discrepancies between noble gas and radionuclide data are not always due to a complex exposure history in the classical sense of collisional fragmentation (Welten et al. 2001b).

THE COSMIC RAY FLUX IN TIME

Concentrations of cosmogenic nuclides in meteorites—as well as in lunar and terrestrial samples—are widely used to study variations in the flux of galactic and solar cosmic radiation over time scales in the range of years to billions of years. GCR flux variations may occur due to variable modulations by the Sun or variations in the intensity of the flux beyond the heliosphere, the region of influence of the Sun. Changes of the interstellar GCR flux may occur, e.g., when the Sun passes through a spiral arm in the Galaxy, where the number of nearby supernovae is higher. In terrestrial samples, variations of the geomagnetic field intensity and several other parameters also have to be considered (Damon and Sonett 1991; Niedermann 2002). This makes meteorites particularly attractive for studying flux variations. On the other hand, radionuclide concentrations in terrestrial reservoirs often provide much higher time resolution, because they record instantaneous, and not integrated, production. Examples are ^{10}Be in sediments or ice cores and ^{14}C in tree rings, which allow, e.g., the study of solar activity during periods of reduced sunspot numbers such as during the Maunder Minimum (Beer et al. 1991; Damon and Sonett 1991).

In meteorites, short-term cosmic ray flux variations can be recognized by measuring the activity of a radionuclide with a short half-life in meteorites with a known fall date. Longer-term variations are studied by comparing apparent production rates of stable (noble gas) nuclides based on various pairs of a stable and a radioactive nuclide, or by comparing experimental and model data (see *Production systematics* subsection).

Short-term variations. Evans et al. (1982) showed that in freshly fallen meteorites between 1967 and 1978 the shielding- and target-chemistry-corrected activities of four radionuclides with half-lives between 16 days and 2.6 years were 2.5-3 times lower at solar maximum than at solar minimum. These data showed that solar modulation of the galactic cosmic radiation by the 11-year solar cycle strongly influences production rates of cosmogenic nuclides. Evans et al. (1982) also noted that their results may suggest variations of solar-modulated cosmic ray fluxes on much longer timescales. A similar variation with the solar cycle between 1965 and 1993 was observed by Bhandari et al. (1994) for the ratio ^{22}Na/^{26}Al, which is rather insensitive to shielding. This result also

implies that a careful correction is needed when applying the couple ^{22}Na-^{22}Ne to determine exposure ages. The radionuclide ^{44}Ti ($T_{1/2} \approx 60$ yr) has been extensively studied by G. Bonino and coworkers in meteorites that fell during the past two hundred years (e.g., Bonino et al. 1999). They find that shielding- and chemistry-corrected ^{44}Ti production rates vary by about 50%. The highest values are observed about 35 years after the two Gleissberg minima of solar activity at ~1800 and ~1900, a phase lag arising because the ^{44}Ti activity at the time of fall represents the time-integrated production rate, not the instantaneous one. Bonino and coworkers note that the ^{44}Ti variations are larger than expected, probably implying that the solar magnetic field during the Gleissberg minima was lower than during recent 11 year cycle minima.

Longer-term variations. Whereas short-term variations are well established and the Sun is known to be their major reason, it is less clear whether meteorites record cosmic ray intensity variations on a million to billion year time scale. The ^{21}Ne production rates derived from the nuclide couple ^{26}Al-^{21}Ne often turned out to be about 50% higher than ^{21}Ne production rates based on other radio-nuclides, in particular ^{22}Na ($T_{1/2} = 2.6$ yr), ^{81}Kr (2.3×10^5 yr), ^{10}Be (1.51×10^6 yr), and ^{53}Mn (3.7×10^6 yr). Such calibrations are discussed by Nishiizumi et al. (1980), Moniot et al. (1983) and earlier studies referenced therein (see *Production systematics* subsection). It is very unlikely that this is due to an incorrectly determined half-life of ^{26}Al. One other possible reason is a higher GCR flux during a time interval for which ^{26}Al is more sensitive than any of the other nuclides studied. As some of these have longer and others shorter half-lives than ^{26}Al, this higher flux would have prevailed perhaps around a few hundred thousand years or so but would have returned to "normal" levels during the more recent periods mainly recorded by ^{81}Kr and ^{22}Na. This is certainly not impossible. Nevertheless, at present a cosmic ray flux change is not the preferred explanation for the aberrant ^{26}Al-based calibration of production rates. A popular explanation is that a large fraction of the meteorites studied with the ^{26}Al-^{21}Ne couple suffered a complex exposure history and hence contain a discernible amount of ^{21}Ne from a first irradiation stage (e.g. Moniot et al. 1983; Vogt et al. 1993). A contribution from an earlier exposure stage contributes more to the total inventory of a stable cosmogenic nuclide if the second stage lasted only briefly (see *Complex Exposure Histories* section). It is therefore to be expected that ^{21}Ne from a previous exposure stage is more easily seen in meteorites with an exposure age short enough that ^{26}Al is not yet in saturation than in meteorites with longer exposures, where ^{10}Be or ^{53}Mn (but not ^{26}Al) are undersaturated. However, according to this logic, complex exposures should compromise nuclide couples involving ^{81}Kr or ^{22}Na even more than those with ^{26}Al. This explanation therefore fails to explain the agreement of the ^{21}Ne production rates based on either ^{81}Kr or ^{22}Na with the values based on ^{10}Be or ^{53}Mn. Vogt et al. (1993) suggest that improper shielding corrections may compromise the ^{26}Al-^{21}Ne system more than the other nuclide couples discussed here.

Fortunately, there is an independent way to use radionuclide concentrations in meteorites to constrain possible temporal variations of the GCR flux. This is by comparing measured nuclide activities in meteorites having a known single-stage exposure history with predicted activites based on data from simulated GCR irradiations and physical nuclide production models (see *Production systematics* subsection). The model by Leya et al. (2000a) does reproduce measured depth profiles of concentrations of ^{10}Be, ^{26}Al, ^{36}Cl, and ^{53}Mn in the chondrite Knyahinya simultaneously using the same assumed value of the GCR flux. This means that the mean cosmic ray flux has been constant to within the combined uncertainties of analyses and model predictions over a few half-lives of the involved radionuclides, i.e., over perhaps 7 to 10 Myr. The range of uncertainty of this statement is somewhat difficult to quantify but should not exceed 30%. Note, however, that the present-day activity of a given nuclide is much more sensitive to

a more recent production rate change than to one of the same magnitude and duration that occurred several half-lives ago. Therefore, if the GCR intensity were higher or lower by 30% earlier than say some 6 Myr ago, this would not be recognized even in the ^{53}Mn activity with present-day precision. To extend the time scale for investigations of the past GCR flux, nuclides with a longer half-life than ^{53}Mn are thus essential. The prime candidate is ^{129}I (15.7 Myr), although only very few data are available so far. Preliminary work by Schnabel et al. (2001) suggests that any change in the GCR flux larger than 35% and 50% over the last 15 and 20 Myr, respectively, is unlikely (see also the discussion of the live ^{129}I-^{129}Xe method in the *Production systematics* subsection*)*.

Beyond ^{129}I, only one radionuclide has been used to study the GCR flux, which is ^{40}K (1.25 Gyr) in iron meteorites (Voshage 1978, 1984 and references therein). This nuclide offers the most firm evidence that the cosmic ray flux may be variable over time scales much longer than those governed by solar activity changes (up to thousands of years), as revealed by meteorites (see above) and ^{10}Be in terrestrial archives (e.g., Beer et al. 1991). Voshage (1984) concluded that the allowed range of ^{21}Ne production rates as a function of ^{4}He/^{21}Ne according to the Signer-Nier model is independent from the ^{40}K-^{41}K ages, indicating that the long-term (~100 Myr or so) average cosmic ray intensity has been constant to within 10-20% over the last 1 Gyr (the exposure age range covered by most iron meteorites). Conversely, by comparing ^{40}K-^{41}K ages with ^{36}Cl-^{36}Ar ages, he concluded that the GCR intensity over the past few Myr (the past few half-lives of ^{36}Cl) was higher than the long-term average by some 50%. Hampel and Schaeffer (1979) arrived at a similar conclusion by comparing ^{26}Al-^{21}Ne ages of iron meteorites with ^{36}Cl-^{36}Ar, ^{39}Ar-^{38}Ar and ^{40}K-^{41}K ages. The ^{36}Cl-^{36}Ar method has recently been systematically applied to iron meteorites by B. Lavielle and coworkers (Lavielle et al. 1999a). These authors confirm a discrepancy between nominal ^{40}K-^{41}K ages and ages based on ^{36}Cl-^{36}Ar or other pairs involving radionuclides with a much shorter half-life than ^{40}K, such as ^{10}Be and ^{53}Mn. In agreement with the conclusions drawn by Voshage, a recent increase of the cosmic ray intensity by some 40% was found to be the most straightforward explanation for this observation, but Lavielle et al. (1999a) caution that the production rate systematics of potassium isotopes may not be known accurately enough to firmly conclude this.

In summary, meteorites provide evidence for GCR flux variations of up to a few times governed by solar activity changes on times scales of 1-100 years. On time scales of up to 5-20 Myr no clear evidence for changes has been found, but in the last 5-20 Myr, and possibly longer, the mean GCR intensity presumably was some 40-50% higher than the average over a billion years. Perhaps this may be explained by the position of the Sun in the Orion arm of the galaxy relatively close to the galactic midplane (Schaeffer 1975). Nothing is known whether such fluctuations on a roughly ten-Myr scale occur regularly, but on a hundred-Myr scale, iron meteorites indicate no discernible GCR flux change.

TERRESTRIAL AGES

Terrestrial ages of meteorites that were not observed to fall are determined with cosmogenic radionuclides, whose production is essentially stopped when the meteorite becomes shielded by terrestrial atmosphere and magnetic field (Jull 2001). Noble gases are used in most such studies only to verify the assumption that the meteorite's exposure age in space was long enough for the radionuclide activity to have reached saturation. However, the radioactive noble gas nuclide ^{81}Kr can also be used to determine terrestrial ages (Freundel et al. 1986; Miura et al. 1993). The most reliable (shielding-corrected) terrestrial ages are obtained by a combined analysis of two or more radionuclides with different half-lives (e.g., ^{36}Cl-^{10}Be, ^{14}C-^{10}Be, ^{41}Ca-^{36}Cl; Nishiizumi et al. 1997a; Lavielle et al. 1999a; Kring et al. 2001; Welten et al. 2001a). The time of fall of a meteorite is

important for studying infall rates, weathering rates, and possible meteorite concentration mechanisms, particularly in areas such as Antarctica or hot deserts where meteorites are actively searched today (Jull 2001). For exposure age determinations using a stable-radioactive nuclide pair, terrestrial ages are also required to correct measured activites of the radionuclide to the time of fall.

COSMOGENIC NOBLE GASES PRODUCED BY SOLAR COSMIC RAYS (SCR)

SCR protons and alpha-particles penetrate only a very few cm into solid matter. Therefore, SCR-produced cosmogenic nuclides are normally not expected to be observed in meteorites, because their outermost few cm usually were ablated in the Earth's atmosphere. SCR nuclide concentration profiles therefore mostly have been calculated for the Moon, i.e., for samples with lunar chemical composition irradiated at 1 AU from the Sun. Most of the recent work has been done by R.C. Reedy and coworkers (e.g., Rao et al. 1994; Reedy 1998a,b) and R. Michel and coworkers (Michel et al. 1996; Neumann 1999). The lunar data also allow one to study temporal variations of SCR fluxes (Reedy and Marti 1991; Reedy 1998b).

In chondrites there is indeed hardly any firm evidence for the presence of SCR noble gases (Garrison et al. 1995). The most promising candidates appear to be small meteorites which hopefully were ablated only little. Indeed a few small meteorites show high levels of ^{26}Al indicative of SCR production (e.g., Nishiizumi et al. 1990), but none of them unequivocally contains SCR-produced ^{21}Ne. Pätsch (2000) reported hints for SCR Ne contributions near the postatmospheric surface for one out of five small Antarctic chondrites studied. It is possible that SCR noble gases may be found near the edges of clasts in meteoritic regolith breccias, i.e., from near-surface samples of pebbles once irradiated in an asteroidal regolith. The few systematic such studies so far have not yielded evidence for SCR noble gases, however (e.g., Wieler et al. 1989b).

One class of martian meteorites, the shergottites, are a very remarkable exception, as all of them show signs of the presence of SCR-Ne in the form of relatively low ^{21}Ne/^{22}Ne ratios (Garrison et al. 1995). In contrast, no representative of the other types of martian meteorites (Chassigny, Nakhlites, ALH84001) shows SCR-Ne. Garrison et al. (1995) suggest that Shergottites may have had atypical orbital parameters compared to other meteorite classes, leading either to a higher production of SCR nuclides relatively close to the Sun or to an atypically low ablation due to low-entry velocities.

Garrison et al. (1995) and Weigel et al. (1999) conclude that SCR-Ne is also present or likely to be present in some acapulcoites and lodranites. For some reason, members of these meteorite classes often had a small preatmospheric size. It should be noted, however, that these conclusions are based on high ^{22}Ne/^{21}Ne ratios of samples without a documented relative position to each other (this is also true for most of the shergottites). A verification by means of depth profiles of ^{21}Ne, ^{22}Ne/^{21}Ne as well as ^{26}Al would be highly desirable.

SCR noble gases have also been found in one iron meteorite (Lavielle et al. 1999b). Arlington has a highly unusual shape that led to a partial preservation of its preatmospheric surface.

ACKNOWLEDGMENTS

I thank Thomas Graf, Bernard Lavielle and Ingo Leya for numerous discussions and suggestions. Ingo Leya and Jozef Masarik kindly provided the data shown in Figures 1-6, Thomas Graf those in Figure 7. Kuni Nishiizumi is acknowledged for his most recent data and compilation of exposure ages of CM and CI chondrites. Very helpful reviews by

Gregory Herzog, Bernard Lavielle, Ingo Leya, Don Porcelli, and Kees Welten are gratefully acknowledged.

REFERENCES

Albrecht A, Schnabel C, Vogt S, Xue S, Herzog GF, Begemann F, Weber HW, Middleton R, Fink D, Klein J (2000) Light noble gases and cosmogenic radionuclides in Estherville, Budulan, and other mesosiderites: Implications for exposure histories and production rates. Meteoritics Planet Sci 35: 975-986

Alexeev VA (1998) Parent bodies of L and H chondrites: Times of catastrophic events. Meteoritics Planet Sci 33 (1):145-152

Anders E (1962) Meteorite ages. Rev Mod Phys 34:287-325

Anders E (1964) Origin, age, and composition of meteorites. Space Sci Rev 3:583-714

Assonov SS, Ivanova MA, Yasevich AN, Shukolyukov YuA (1996) Dengli H3.8 chondrite noble gases: Evidence of the regolith nature of brecciation and of two-stage cosmic irradiation. Geochem Intl 34:825-833

Aylmer D, Vogt S, Herzog GF, Klein J, Fink D, Middleton R (1990) Low ^{10}Be and ^{26}Al contents of ureilites: Production at meteoroid surfaces. Geochim Cosmochim Acta 54:1775-1784

Beer J, Raisbeck GM, Yiou F (1991) Time variations of Be-10 and solar activity. *In* The Sun in Time. Sonett CP, Giampapa MS, Matthews MS (eds) Univ. Arizona Press, Tucson, p 343-359

Begemann F, Schultz L (1988) The influence of bulk chemical composition on the production rate of cosmogenic nuclides in meteorites. Lunar Planet Sci IXX, Lunar Planet Institute, Houston, p 51-52

Begemann F, Geiss J, Hess DC (1957) Radiation age of a meteorite from cosmic-ray-produced He^3 and H^3. Phys Rev 107:540-542

Begemann F, Weber HW, Vilcsek E, Hintenberger H (1976) Rare gases and ^{36}Cl in stony-iron meteorites: cosmogenic elemental production rates, exposure ages, diffusion losses and thermal histories. Geochim Cosmochim Acta 40:353-368

Begemann F, Fan CY, Weber HW, Wang XB (1996) Light noble gases in Jilin: More of the same and something new. Meteoritics Planet Sci 31:667-674.

Benoit PH, Sears DWG (1997) The orbits of meteorites from natural thermoluminescence. Icarus 125: 281-287.

Bhandari N, Bonino G, Cini Castagnoli G (1994) The 11-year solar cycle variation of cosmogenic isotope production rates in chondrites. Meteoritics 29:443-444

Bhattacharya SK, Goswami JN, Lal D (1973) Semiempirical rates of formation of cosmic ray tracks in spherical objects exposed in space: preatmospheric and postatmospheric depth profiles. J Geophys Res 78:8356-8363

Binzel RP, Xu S (1993) Chips off of Asteroid-4 Vesta—evidence for the parent body of basaltic achondrite meteorites. Science 260:186-191

Blann M (1971) Hybrid model for pre-equilibrium decay in nuclear reactions. Phys Rev Lett 27: 337 - 340

Bogard DD (1995) Impact ages of meteorites: A synthesis. Meteoritics 30:244-268

Bogard DD, Cressy PJ (1973) Spallation production of ^{3}He, ^{21}Ne, and ^{38}Ar from target elements in the Bruderheim chondrite. Geochim Cosmochim Acta 37:527-546

Bogard DD, Nyquist LE, Bansal BM, Garrison DH, Wiesmann H, Herzog GF, Albrecht AA, Vogt S, Klein J (1995) Neutron-capture ^{36}Cl, ^{41}Ca, ^{36}Ar, and ^{150}Sm in large chondrites: Evidence for high fluences of thermalized neutrons. J Geophys Res E100:9401-9416

Bogard DD, Garrison DH, Masarik J (2001) The Monahans chondrite and halite: Argon-39/argon-40 age, solar gases, cosmic ray exposure ages, and parent body regolith neutron flux and thickness. Meteoritics Planet Sci 36:107-122

Bonino G, Cini Castagnoli G, Bhandari N, Della Monica P, Taricco C (1999) Galactic cosmic ray variations in the last two centuries recorded by cosmogenic ^{44}Ti in meteorites. Adv Space Res 23: 607-610

Bottke WF, Rubincam DP, Burns JA (2000) Dynamical evolution of main belt meteoroids: Numerical simulations incorporating planetary perturbations and Yarkovsky thermal forces. Icarus 145:301-331

Caffee MW, Nishiizumi K (1997) Exposure ages of carbonaceous chondrites: II. Meteoritics Planet Sci 32:A26

Caffee MW, Nishiizumi K (2001) Exposure history of separated phases from the Kapoeta meteorite. Meteoritics Planet Sci 36:429-437

Caffee MW, Goswami JN, Hohenberg CM, Swindle TD (1983) Cosmogenic neon from precompaction irradiation of Kapoeta and Murchison. Proc Lunar Planet Sci Conf 14th:B267-B273

Caffee MW, Hohenberg CM, Swindle TD, Goswami JN (1987) Evidence in meteorites for an active early Sun. Astrophys J 313:L31-L35

Damon PE, Sonett CP (1991) Solar and terrestrial components of the atmospheric ^{14}C variation spectrum. *In* The Sun in Time. Sonett CP, Giampapa MS, Matthews MS (eds) Univ. Arizona Press, Tucson, p 360-388

Eberhardt P, Geiss J, Lutz H (1963) Neutrons in meteorites. *In* Earth Science and Meteoritics. Geiss J, Goldberg ED (eds) North Holland, Amsterdam, p 143-168

Eberhardt P, Eugster O, Geiss J (1965) Radiation ages of aubrites. J Geophys Res 70:4427-4434

Eberhardt P, Eugster O, Geiss J, Marti K (1966) Rare gas measurements in 30 stone meteorites. Z Naturf 21a:414-426

Eberhardt P, Geiss J, Graf H (1971) On the origin of excess ^{131}Xe in lunar rocks. Earth Planet Sci Lett 12:260-262

Eugster O (1988) Cosmic ray production rates for ^{3}He, ^{21}Ne, ^{38}Ar, ^{83}Kr, and ^{126}Xe in chondrites based on ^{81}Kr-Kr exposure ages. Geochim Cosmochim Acta 52:1649-1662

Eugster O, Michel T (1995) Common asteroid break-up events of eucrites, diogenites, and howardites and cosmic ray production rates for noble gases in achondrites. Geochim Cosmochim Acta 59:177-199

Eugster O, Eberhardt P, Geiss J (1969) Isotopic analyses of krypton and xenon in fourteen stone meteorites. J Geophys Res 74:3874-3896

Eugster O, Tera F, Burnett DS, Wasserburg GJ (1970) Isotopic composition of gadolinium and neutron-capture effects in some meteorites. J Geophys Res 75:2753-2768

Eugster O, Eberhardt P, Thalmann C, Weigel A (1998a) Neon-E in CM-2 chondrite LEW90500 and collisional history of CM-2 chondrites, Maralinga, and other CK chondrites. Geochim Cosmochim Acta 62:2573-2582

Eugster O, Polnau E, Terribilini D (1998b) Cosmic ray- and gas retention ages of newly recovered and of unusual chondrites. Earth Planet Sci Lett 164:511-519

Evans JC, Reeves JH, Rancitelli LA, Bogard DD (1982) Cosmogenic nuclides in recently fallen meteorites: evidence for galactic cosmic ray variations during the period 1967-1978. J Geophys Res 87:5577-5591

Farinella P, Vokrouhlicky D, Morbidelli A (2001) Delivery of material from the asteroid belt. *In* Accretion of extraterrestrial matter throughout Earth's history. Peucker-Ehrenbrink B, Schmitz B (eds) Kluwer, New York, p 31-49

Finkel RC, Kohl CP, Marti M, Martinek B, Rancitelli L (1978) The cosmic ray record in the San Juan Capistrano meteorite. Geochim Cosmochim Acta 42:241-250

Fleischer RL, Price PB, Walker RM. (1975) Nuclear tracks in solids. Univ. California Press, Berkeley

Freundel M, Schultz L, Reedy RC (1986) Terrestrial ^{81}Kr-Kr ages of Antarctic meteorites. Geochim Cosmochim Acta 50:2663-2673

Garrison DH, Bogard DD, Albrecht AA, Vogt S, Herzog GF, Klein J, Fink D, Dezfouly-Arjomandy B, Middleton R (1992) Cosmogenic nuclides in core samples of the Chico L6-chondrite—evidence for irradiation under high shielding. Meteoritics 27:371-381

Garrison DH, Rao MN, Bogard DD (1995) Solar-proton-produced neon in shergottite meteorites and implications for their origin. Meteoritics 30:738-747

Gladman B (1997) Destination: Earth. Martian meteorite delivery. Icarus 130:228-246

Gladman BJ, Burns JA, Duncan M, Lee P, Levison HF (1996) The exchange of impact ejecta between terrestrial planets. Science 271:1387-1392

Gladman BJ, Migliorini F, Morbidelli A, Zappala V, Michel P, Cellino A, Froeschle C, Levison HF, Bailey M, Duncan M (1997) Dynamical lifetimes of objects injected into asteroid belt resonances. Science 277:197-201

Göbel R, Bergmana F, Ott U (1982) On neutron-induced and other noble gases in Allende inclusions. Geochim Cosmochim Acta 46:1777-1792

Goodrich CA (1992) Ureilites—A critical review. Meteoritics 27:327-352

Graf T, Marti K (1994) Collisional records in LL-chondrites. Meteoritics 29:643-648

Graf T, Marti K (1995) Collisional history of H chondrites. J Geophys Res E100:21247-21263

Graf T, Vogt S, Bonani G, Herpers U, Signer P, Suter M, Wieler R, Wölfli W (1987) Depth dependence of ^{10}Be and ^{26}Al production in the iron meteorite Grant. Nucl Instr Methods B29:262-265

Graf T, Baur H, Signer P (1990a) A model for the production of cosmogenic nuclides in chondrites. Geochim Cosmochim Acta 54:2521-2534

Graf T, Signer P, Wieler R, Herpers U, Sarafin R, Vogt S, Fiéni C, Pellas P, Bonani G, Suter M, Wölfli W (1990b) Cosmogenic nuclides and nuclear tracks in the chondrite Knyahinya. Geochim Cosmochim Acta 54:2511-2520

Graf T, Caffee MW, Marti K, Nishiizumi K, Ponganis KV (2001) Dating collisional events: ^{36}Cl-^{36}Ar exposure ages of H-chondritic metals. Icarus 150:181-188

Greenberg R, Nolan MC (1989) Delivery of asteroids and meteorites to the inner solar system. *In* Asteroids II. Binzel RP, Gehrels T, Matthews MS (eds) Univ. Arizona Press, Tucson, p 778-804

Hampel W, Schaeffer OA (1979) ^{26}Al in iron meteorites and the constancy of cosmic ray intensity in the past. Earth Planet Sci Lett 42:348-358

Herzog GF, Anders E (1971) Absolute scale for radiation ages of stony meteorites. Geochim Cosmochim Acta 35:605-611

Herzog GF, Vogt S, Albrecht A, Xue S, Fink D, Klein J, Middleton R, Weber HW, Schultz L (1997) Complex exposure histories for meteorites with short exposure ages. Meteoritics Planet Sci 32: 413-422.

Heusser G, Ouyang Z, Oehm J, Yi W (1996) Aluminum-26, sodium-22 and cobalt-60 in two drill cores and some other samples of the Jilin chondrite. Meteoritics Planet Sci 31:657-665.

Heymann D (1967) On the origin of hypersthene chondrites: ages and shock effects of black chondrites. Icarus 6:189-221

Heymann D, Lipschutz ME, Nielsen B, Anders E (1966) Canyon Diablo meteorite: metallographic and mass spectrometric study of 56 fragments. J Geophys Res 71:619-641

Hidaka H, Ebihara M, Yoneda S (1999) High fluences of neutrons determined from Sm and Gd isotopic compositions in aubrites. Earth Planet Sci Lett 173:41-51

Hidaka H, Yoneda S, Nishiizumi K (2001) Neutron capture effects on Sm and Gd isotopes in Martian meteorites. Meteoritics Planet Sci 36:A80-A81

Hohenberg CM, Marti K, Podosek FA, Reedy RC, Shirck JR (1978) Comparisons between observed and predicted cosmogenic noble gases in lunar samples. Proc Lunar Planet Sci Conf 9th:2311-2344

Hohenberg CM, Hudson B, Kennedy BM, Podosek FA (1981) Xenon spallation systematics in Angra dos Reis. Geochim Cosmochim Acta 45:1909-1915

Hohenberg CM, Nichols RH, Olinger CT, Goswami JN (1990) Cosmogenic neon from individual grains of CM meteorites: Extremely long pre-compaction exposure histories or an enhanced early particle flux. Geochim Cosmochim Acta 54:2133-2140

Honda M (1988) Statistical estimation of the production of cosmic-ray-induced nuclides in meteorites. Meteoritics 23:3-12

Jull AJT (2001) Terrestrial ages of meteorites. *In* Accretion of extraterrestrial matter throughout Earth's history. Peucker-Ehrenbrink B, Schmitz B (eds). Kluwer, New York, p 241-266

Jull AJT, Donahue DJ, Reedy RC, Masarik J (1994) A Carbon-14 depth profile in the L5 chondrite Knyahinya. Meteoritics 29:649-651

Kallemeyn GW, Rubin AE, Wasson JT (1991) The compositional classification of chondrites: V. The Karoonda (CK) group of carbonaceous chondrites. Geochim Cosmochim Acta 55:881-892

Keil K (1989) Enstatite meteorites and their parent bodies. Meteoritics 24:195-208

Keil K, Haack H, Scott ERD (1994) Catastrophic fragmentation of asteroids: Evidence from meteorites. Planet Space Sci 42:1109-1122

Kim JS, Marti K (1992) Solar-type xenon: isotopic abundances in Pesyanoe. Proc Lunar Planet Sci 22: 145-151

Kring DA, Jull AJT, McHargue LR, Bland PA, Hill DH, Berry FJ (2001) Gold Basin meteorite strewn field, Mojave Desert, northwestern Arizona: Relic of a small late Pleistocene impact event. Meteoritics Planet Sci 36:1057-1066

Kohl CP, Murrell MT, Russ GP, Arnold JR (1978) Evidence for the constancy of the solar cosmic ray flux over the past ten million years: ^{53}Mn and ^{26}Al measurements. Proc Lunar Planet Sci Conf 9th: 2299-2310

Lavielle B, Marti K (1988) Cosmic ray produced Kr in St. Severin core AIII. Proc Lunar Planet Sci Conf 18th:565-572

Lavielle B, Regnier S, Marti K (1985) Ages d'exposition des météorites de fer: histoires multiples et variations d'intensité du rayonnement cosmique. *In* Isotopic ratios in the solar system, Cepadues-Editions, Toulouse, France:15-20

Lavielle B, Toe S, Gilabert E (1997) Noble Gas Measurements In the L/LL5 Chondrite Knyahinya. Meteoritics Planet Sci 32:97-107.

Lavielle B, Marti K, Jeannot JP, Nishiizumi K, Caffee M (1999a) The Cl-36-Ar-36-K-40-K-41 records and cosmic ray production rates in iron meteorites. Earth Planet Sci Lett 170:93-104

Lavielle B, Gilabert E, Marti K (1999b) Records of solar energetic particles in the iron meteorite Arlington. Meteoritics Planet Sci 34:A72-A73

Lavielle B, Gilabert E, Marti K, Nishiizumi K, Caffee MW (2000) Collisional history in irons: interpreting the cosmic ray record. Meteoritics Planet Sci 35:A96

Lavielle B, Caffee MW, Gilabert E, Marti K, Nishiizumi K, Ponganis KV (2001) Irradiation records in Group IVA irons. Meteoritics Planet Sci 36:A110-A111

Lewis RS, Amari S, Anders E (1994) Interstellar grains in meteorites: II. SiC and its noble gases. Geochim Cosmochim Acta 58:471-494

Leya I (1997) Modellrechnungen zur Beschreibung der Wechselwirkungen galaktischer kosmischer Teilchenstrahlung mit Stein- und Eisenmeteoroiden. PhD thesis, University of Hannover

Leya I, Michel R (1997) Determination of neutron cross sections for nuclide production at intermediate energies by deconvolution of thick-target production rates. *In* Proc Int Conf Nuclear Data for Science and Technology. Reffo G (ed) Trieste, Italy, p 1463-1467

Leya I, Lange HJ, Neumann S, Wieler R, Michel R (2000a) The production of cosmogenic nuclides in stony meteoroids by galactic cosmic ray particles. Meteoritics Planet Sci 35:259-286

Leya I, Lange HJ, Lüpke M, Neupert U, Daunke R, Fanenbruck O, Michel R, Rösel R, Meltzow B, Schiekel T, Sudbrock F, Herpers U, Filges D, Bonani G, Dittrich Hannen B, Suter M, Kubik PW, Synal HA (2000b) Simulation of the interaction of galactic cosmic ray protons with meteoroids: On the production of radionuclides in thick gabbro and iron targets irradiated isotropically with 1.6 GeV protons. Meteoritics Planet Sci 35:287-318

Leya I, Wieler R, Halliday AN (2000c) Cosmic ray production of tungsten isotopes in lunar samples and meteorites and its implications for Hf-W cosmochemistry. Earth Planet Sci Lett 175:1-12

Leya I, Graf T, Nishiizumi K, Wieler R (2001a) Cosmic-ray production rates of helium, neon and argon isotopes in H chondrites based on chlorine-36/argon-36 ages. Meteoritics Planet Sci 36:963-973

Leya I, Neumann S, Wieler R, Michel R (2001b) The production of cosmogenic nuclides by GCR-particles for 2π exposure geometries. Meteoritics Planet Sci 36:1547-1561

Lingenfelter RE, Canfield EH, Hampel VE (1972) The lunar neutron flux revisited. Earth Planet Sci Lett 16:355-369

Loeken T, Scherer P, Weber HW, Schultz L (1992) Noble gases in eighteen stone meteorites. Chem Erde 52:249-259

Lorenzetti S, Eugster O, Burbine T, McCoy TJ, Marti K (2001) Break-up events on the aubrite parent body. Meteoritics Planet Sci 36:A116-A117

Lugmair GW, Marti K (1971) Neutron capture effects in lunar gadolinium and the irradiation histories of some lunar rocks. Earth Planet Sci Lett 13:32-42

Ma P, Herzog GF, Faestermann T, Knie K, G. Korschinek (2001) ^{53}Mn activities and ^{26}Al-^{53}Mn exposure ages of lodranites and acapulcoites. Meteoritics Planet Sci 36:A120

Marti K (1967) Mass-spectrometric detection of cosmic-ray-produced Kr^{81} in meteorites and the possibility of Kr-Kr dating. Phys Rev Lett 18:264-266

Marti K, Lugmair GW (1971) Kr^{81}-Kr and K-Ar^{40} ages, cosmic ray spallation products, and neutron effects in lunar samples from Oceanus Procellarum. Proc Lunar Sci Conf 2nd:1591-1605

Marti K, Graf T (1992) Cosmic ray exposure history of ordinary chondrites. Ann Rev Earth Planet Sci 20:221-243

Marti K, Murty SVS, Nishiizumi K. (1986) Neutron exposure age of the Cape York iron meteorite. Lunar Planet Sci XVII, Lunar Planet Institute, Houston:516-517.

Masarik J, Reedy RC (1994) Effects of bulk composition on nuclide production processes in meteorites. Geochim Cosmochim Acta 58:5307-5317

Masarik J, Nishiizumi K, Reedy RC (2001) Production rates of cosmogenic ^{3}He, ^{21}Ne, and ^{22}Ne in ordinary chondrites and the lunar surface. Meteoritics Planet Sci 36:643-650

McCoy TJ, Keil K, Clayton RN, Mayeda TK, Bogard DD, Garrison DH, Wieler R (1997) A petrologic and isotopic study of lodranites: evidence for early formation as partial melt residues from heterogeneous precursors. Geochim Cosmochim Acta 61:623-637

Merchel S, Altmaier M, Faestermann T, Herpers U, Knie K, Korschinek G, Kubik PW, Neumann S, Michel R, Suter M (1999) Saharan meteorites with short or complex exposure histories. *In* Workshop on extraterrestrial materials from cold and hot deserts. Lunar Planet. Institute, Houston, Contrib No. 997:53-56

Michel R, Dragovitsch P, Englert P, Peiffer F, Stück R, Theis S, Begemann F, Weber HW, Signer P, Wieler R, Filges D, Cloth P (1986) On the depth dependence of spallation reactions in a spherical thick diorite target homogeneously irradiated by 600 MeV protons. Simulation of production of cosmogenic nuclides in small meteorites. Nucl Instr Methods B16:61-82

Michel R, Leya I, Borges L (1996) Production of cosmogenic nuclides. *In* Meteoroids: accelerator experiments and model calculations to decipher the cosmic ray record in extraterrestrial matter. Nucl Instr Methods B 113:434-444

Michlovich ES, Vogt S, Masarik J, Reedy RC, Elmore D, Lipschutz ME (1994) Aluminum 26, ^{10}Be, and ^{36}Cl depth profiles in the Canyon Diablo iron meteorite. J Geophys Res 99:23187-23194

Miura Y, Nagao K, Fujitani T (1993) ^{81}Kr terrestrial ages and grouping of Yamato eucrites based on noble gas and chemical compositions. Geochim Cosmochim Acta 57:1857-1866

Miura YN, Nagao K, Okazaki R (2000) Noble gas studies of aubrites. Meteoritics Planet Sci 35:A112

Moniot RK, Kruse TH, Tuniz C, Savin W, Hall GS, Milazzo T, Pal D, Herzog GF (1983) The ^{21}Ne production rate in stony meteorites estimated from ^{10}Be and other radionuclides. Geochim Cosmochim Acta 47:1887-1895

Morbidelli A, Gladman B (1998) Orbital and temporal distributions of meteorites originating in the asteroid belt. Meteoritics Planet Sci 33:999-1016

Neumann S (1999) Aktivierungsquerschnitte mit Neutronen mittlerer Energien und die Produktion kosmogener Nuklide in extraterrestrischer Materie. PhD dissertation, University of Hannover

Niedermann S (2002) Cosmic-ray-produced noble gases in terrestrial rocks as a dating tool for surface processes. Rev Mineral Geochem 47:731-784

Nishiizumi K (1987) ^{53}Mn, ^{26}Al, ^{10}Be and ^{36}Cl in meteorites: data compilation. Nucl Tracks Radiat Meas 13:209-273

Nishiizumi K, Caffee MW (2001) Exposure histories of lunar meteorites Dhofar 025, 026, and Northwest Africa 482. Meteoritics Planet Sci 36:A148-A149

Nishiizumi K, Regnier S, Marti K (1980) Cosmic ray exposure ages of chondrites, pre-irradiation and constancy of cosmic ray flux in the past. Earth Planet Sci Lett 50:156-170

Nishiizumi K, Nagai H, Imamura M, Honda M, Kobayashi K, Kubik PW, Sharma P, Wieler R, Signer P, Goswami JN, Reedy RC, Arnold JR (1990) Solar cosmic ray produced nuclides in Salem meteorite. Meteoritics 25:392

Nishiizumi K, Arnold JR, Caffee MW, Finkel RC, Southon JR, Nagai H, Honda M, Imamura M, Kobayashi K, Sharma P (1993) Exposure ages of carbonaceous chondrites—I. Lunar Planet Sci XXIV; Lunar Planet Institute, Houston:1085-1086

Nishiizumi K, Caffee MW, Jeannot J-P, Lavielle B, Honda M (1997a) A systematic study of the cosmic-ray-exposure history of iron meteorites: Beryllium-10-chlorine-36/beryllium-10 terrestrial ages. Meteoritics Planet Sci 32:A100

Nishiizumi K, Fink D, Klein J, Middleton R, Masarik J, Reedy RC, Arnold JR (1997b) Depth profile of ^{41}Ca in an Apollo 15 drill core and the low-energy neutron flux in the Moon. Earth Planet Sci Lett 148:545-552

Nishiizumi K, Masarik J, Caffee MW, Jull AJT (1999) Exposure histories of pair lunar meteorites EET 96008 and EET 87521. Lunar Planet Sci Conf XXX, Lunar Planet Institute, Houston, TX, Abstr #1980, CD-ROM

Nishiizumi K, Caffee MW, Masarik J (2000) Cosmogenic radionuclides in the Los Angeles Martian meteorite. Meteoritics Planet Sci 35:A120

Nyquist LE, Borg LE, Shih CY (1998) The Shergottite age paradox and the relative probabilities for Martian meteorites of differing ages. J Geophys Res E103:31445-31455

Nyquist LE, Bogard DD, Shih C-Y, Greshake A, Stöffler D, Eugster O (2001) Ages and geologic histories of martian meteorites. Space Sci Rev 96:105-164

Olinger CT, Maurette M, Walker RM, Hohenberg CM (1990) Neon measurements of individual Greenland sediment particles: proof of an extraterrestrial origin. Earth Planet Sci Lett 100:77-93

Olsen E, Davis A, Clarke RS, Schultz L, Weber HW, Clayton R, Mayeda T, Jarosewich E, Sylvester P, Grossman L, Wang MS, Lipschutz ME, Steele IM, Schwade J (1994) Watson—a new link in the IIE iron chain. Meteoritics 29:200-213

Ott U (2002) Noble gases in meteorites—trapped components. Rev Mineral Geochem 47:71-100

Ott U, Begemann F (2000) Spallation recoil and age of presolar grains in meteorites. Meteoritics Planet Sci 35:53-63

Ott U, Altmeier M, Herpers U, Kuhnhenn J, Merchel S, Michel R, Mohapatra RK (2001) Update on recoil loss of spallation products from presolar grains. Meteoritics Planet Sci 36:A155-A156

Okazaki R, Takaoka N, Nakamura T, Nagao K (2000) Cosmic ray exposure ages of enstatite chondrites. Antarct Meteorite Res (Natl Inst Polar Research, Tokyo) 13:153-169

Pätsch M. (2000) Produkte der Solaren Kosmischen Strahlung in Meteoriten: Aufbau und Erprobung einer Laser-Extraktionsanlage für Edelgase. PhD Thesis, Johannes Gutenberg Universität, Mainz.

Patzer A, Schultz L (2001) Noble gases in enstatite chondrites I: exposure ages, pairing, and weathering effects. Meteoritics Planet Sci 36:947-961

Pedroni A (1989) Die korpuskulare Bestrahlung der Oberflächen von Asteroiden; eine Studie der Edelgase in den Meteoriten Kapoeta und Fayetteville. PhD dissertation, ETH Zürich, Nr. 8880.

Pepin RO, Becker RH, Rider PE (1995) Xenon and krypton isotopes in extraterrestrial regolith soils and in the solar wind. Geochim Cosmochim Acta 59:4997-5022

Pellas P, Fiéni C (1988) Thermal histories of ordinary chondrite parent asteroids. Lunar Planet Sci XIX, Lunar Planetary Institute, Houston, p 915-916

Polnau E, Eugster O (1998) Cosmic ray produced, radiogenic, and solar noble gases in lunar meteorites Queen Alexandra Range 94269 and 94281. Meteoritics Planet Sci 33:313-319

Polnau E, Eugster O, Krähenbühl U, Marti K (1999) Evidence for a precompaction exposure to cosmic rays in a chondrule from the H6 chondrite ALH76008. Geochim Cosmochim Acta 63:925-933

Polnau E, Eugster O, Burger M, Krähenbühl U, Marti K (2001) Precompaction exposure of chondrules and implications. Geochim Cosmochim Acta 65:1849-1866

Pun A, Keil K, Taylor GJ, Wieler R (1998) The Kapoeta howardite: Implications for the regolith evolution of the HED parent body. Meteoritics Planet Sci 33:835-851

Raisbeck GM, Yiou F (1989) Cosmic ray exposure ages of cosmic spherules. Meteoritics 24:318

Rao MN, Garrison DH, Bogard DD, Reedy RC (1994) Determination of the flux-distribution and energy-distribution of energetic solar protons in the past 2-Myr using lunar rock- 68815. Geochim Cosmochim Acta 58:4231-4245

Reedy RC (1981) Cosmic-ray-produced stable nuclides: Various production rates and their implications. Proc Lunar Planet Sci, 12B:1809-1823

Reedy RC (1998a) Studies of modern and ancient solar energetic particles. Proceedings Indian Acad Sci–Earth Planetary Sci 107:433-440

Reedy RC (1998b) Variations in solar-proton fluxes over the last million years. Meteoritics Planet Sci 33:A127-A127

Reedy RC, Marti M (1991) Solar-cosmic ray fluxes during the last ten million years. *In* The Sun in time. Sonett CP, Giampapa MS, Matthews MS (eds) Univ Arizona Press, Tucson, p 260-287

Reedy RC, Arnold JR, Lal D (1983) Cosmic ray record in solar system matter. Ann Rev Nucl Part Sci 33:505-537

Reedy RC, Masarik J, Nishiizumi K, Arnold JR, Finkel RC, Caffee MW, Southon J, Jull AJT, Donahue DJ (1993) Cosmogenic-radionuclide profiles in Knyahinya: new measurements and models. Lunar Planet Sci XXIV; Lunar Planet Institute, Houston, p 1195-1196

Regnier S, Hohenberg CM, Marti K, Reedy RC (1979) Predicted versus observed cosmic ray produced noble gases in lunar samples: Improved Kr production ratios. Proc Lunar Planet Sci Conf 10th: 1565-1586

Sands DG, De Laeter JR, Rosman KJR (2001) Measurements of neutron capture effects on Cd, Sm and Gd in lunar samples with implications for the neutron energy spectrum. Earth Planet Sci Lett 186:335-346

Schaeffer OA (1975) Constancy of galactic cosmic rays in time and space. 14th Intl Cosmic Ray Conf: 3508-3520

Schaeffer OA, Nagel K, Fechtig H, Neukum G (1981) Space erosion of meteorites and the secular variation of cosmic rays (over 10^9 years). Planet Space Sci 29:1109-1118

Scherer P, Schultz L (2000) Noble gas record, collisional history, and pairing of CV, CO, CK, and other carbonaceous chondrites. Meteoritics Planet Sci 35:145-153

Scherer P, Zipfel J, Schultz L (1998) Noble gases in two new ureilites from the Saharan desert. Lunar Planet Sci XXIX, Lunar Planet Institute, Houston, TX:Abstr #1383 (CD ROM)

Schnabel C, Leya I, Wieler R, Herd RK, Synal H-A, Krähenbühl U, Herzog GF (2001) ^{129}I in Knyahinya and Abee and a first estimate of GCR constancy over 20 Myr. Meteoritics Planet Sci 36:A183-A184

Schultz L, Signer P (1976) Depth dependence of spallogenic helium, neon, and argon in the St. Severin chondrite. Earth Planet Sci Lett 30:191-199

Schultz L, Signer P (1977) Noble gases in the St. Mesmin chondrite: Implications to the irradiation history of a brecciated meteorite. Earth Planet Sci Lett 36:363-371

Schultz L, Franke L (2000) Helium, neon, and argon in meteorites-a data collection, update 2000. Max-Planck-Institut für Chemie, Mainz, CD-ROM (Schultz@mpch-mainz.mpg.de)

Schultz L, Weber HW (2001) The irradiation history of Rumuruti-chondrites. 26th Symp Antarctic Meteorites, Natl Inst Polar Research, Tokyo, p 128-130

Schultz L, Weber HW, Begemann F (1991) Noble gases in H-chondrites and potential differences between Antarctic and non-Antarctic meteorites. Geochim Cosmochim Acta 55:59-66

Signer P, Nier AO (1960) The distribution of cosmic-ray-produced rare gases in iron meteorites. J Geophys Res 65:2947-2964

Signer P, Nier AO (1962) The measurement and interpretation of rare gas concentrations in iron meteorites. *In* Researches in meteorites. Moore CB (ed) John Wiley & Sons, New York, p 7-35

Sisterson JM, Jones DTL, Binns PJ, Langen K, Schroeder I, Buthelezi Z, Latti E, Brooks FD, Buffler A, Allie MS, Herbert MS, Nchodu MR, Makupula S, Ullmann J, Reedy RC (2001) Production of ^{22}Na and other radionuclides by neutrons in Al, SiO_2, Si, Ti, Fe and Ni targets: implications for cosmic ray studies. Lunar Planet Sci, XXXII, Lunar & Planetary Institute, Houston, Abstr #1302,CD-ROM

Spergel MS, Reedy RC, Lazareth OW, Levy PW, Slatest LA (1986) Cosmogenic neutron-capture-produced nuclides in stony meteorites. Proc Lunar Planet Sci Conf 16th:D483-D494

Swindle TD (2002a) Noble gases in the Moon and meteorites: Radiogenic components and early volatile chronologies. Rev Mineral Geochem 47:101-124

Swindle TD (2002b) Martian noble gases. Rev Mineral Geochem 47:171-190

Terribilini D, Eugster O, Herzog GF, Schnabel C (2000a) Evidence for common breakup events of the acapulcoites-lodranites and chondrites. Meteoritics Planet Sci 35:1043-1050

Terribilini D, Eugster O, Mittlefehldt DW, Diamond LW, Vogt S, Wang D (2000b) Mineralogical and chemical composition and cosmic ray exposure history of two mesosiderites and two iron meteorites. Meteoritics Planet Sci 35:617-628

Tuniz C, Bird JR, Fink D, Herzog GF. (1998) Accelerator Mass Spectrometry. CRC Press, Boca Raton, Florida

Vogt S, Herzog GF, Reedy RC (1990) Cosmogenic nuclides in extraterrestrial materials. Rev Geophys 28:253-275

Vogt SK, Aylmer D, Herzog GF, Wieler R, Signer P, Pellas P, Fiéni C, Tuniz C, Jull AJT, Fink D, Klein J, Middleton R (1993) On the Bur Gheluai H5 chondrite and other meteorites with complex exposure histories. Meteoritics 28:71-85

Voshage H (1978) Investigations on cosmic-ray-produced nuclides in iron meteorites, 2. New results on $^{41}K/^{40}K$-$^{4}He/^{21}Ne$ exposure ages and the interpretations of age distributions. Earth Planet Sci Lett 40:83-90

Voshage H (1984) Investigations of cosmic-ray-produced nuclides in iron meteorites, 6. The Signer-Nier model and the history of the cosmic radiation. Earth Planet Sci Lett 71:181-194

Warren PH (1994) Lunar and Martian meteorite delivery services. Icarus 111:338-363

Warren PH (2001) Porosities of lunar meteorites: Strength, porosity, and petrologic screening during the meteorite delivery process. J Geophys Res E106:10101-10111

Wasson JT (1990) Ungrouped iron meteorites in Antarctica: origin of anomalously high abundance. Science 249:900-902

Wasson JT (1995) Sampling the asteroid belt: how biases make it difficult to establish meteorite-asteroid connections. Meteoritics 30:595

Weigel A, Eugster O, Koeberl C, Michel R, Krähenbühl U, Neumann S (1999) Relationships among lodranites and acapulcoites: Noble gas isotopic abundances, chemical composition, cosmic ray exposure ages, and solar cosmic ray effects. Geochim Cosmochim Acta 63:175-192

Welten KC, Lindner L, van der Borg K, Loeken T, Scherer P, Schultz L (1997) Cosmic ray exposure ages of diogenites and the recent collisional history of the howardite, eucrite and diogenite parent body/bodies. Meteoritics Planet Sci 32:891-902

Welten KC, Nishiizumi K, Masarik J, Caffee MW, Jull AJT, Klandrud SE, Wieler R (2001a) Cosmic ray exposure history of two Frontier Mountain H-chondrite showers from spallation and neutron-capture products. Meteoritics Planet Sci 36:301-317

Welten KC, Nishiizumi K, Caffee MW, Schultz L (2001b) Update on exposure ages of diogenites: the impact history of the HED parent body and evidence of space erosion and/or collisional disruption of stony meteoroids. Meteoritics Planet Sci 36:A223

Welten KC, Bland PA, Russell SS, Grady MM, Caffee MW, Masarik J, Jull AJT, Weber HW, Schultz L (2001c) Exposure age, terrestrial age and pre-atmospheric radius of the Chinguetti mesosiderite: Not part of a much larger mass. Meteoritics Planet Sci 36:939-946

Welten KC, Nishiizumi K, Caffee MW (2001d) The search for meteorites with complex exposure histories among ordinary chondrites with low $^{3}He/^{21}Ne$ ratios. Lunar Planet Sci XXXII, Abstr #2148 (CD-ROM).

Welten KC, Nishiizumi K, Caffee MW, Masarik J, Wieler R (2001e) A complex exposure history of the Gold Basin L4-chondrite shower from cosmogenic radionuclides and noble gases. Lunar Planet Sci XXXII, Abstr #2110 (CD-ROM).

Wetherill GW, Williams JG (1979) Origin of differentiated meteorites. *In* Origin and distribution of the elements. Ahrens LH (ed) Pergamon, Oxford, p19-31

Wieler R (2002) Noble gases in the solar system. Rev Mineral Geochem 47:21-70

Wieler R, Graf T (2001) Cosmic ray exposure history of meteorites. *In* Accretion of extraterrestrial matter throughout Earth's history. Peucker-Ehrenbrink B, Schmitz B (eds) Kluwer, New York, p 221-240

Wieler R, Baur H, Pedroni A, Signer P, Pellas P (1989a) Exposure history of the regolithic chondrite Fayetteville: I. Solar-gas-rich matrix. Geochim Cosmochim Acta 53:1441-1448

Wieler R, Graf T, Pedroni A, Signer P, Pellas P, Fiéni C, Suter M, Vogt S, Clayton RN, Laul JC (1989b) Exposure history of the regolithic chondrite Fayetteville: II. Solar-gas-free light inclusions. Geochim Cosmochim Acta 53:1449-1459

Wieler R, Graf T, Signer P, Vogt S, Herzog GF, Tuniz C, Fink D, Fifield LK, Klein J, Middleton R, Jull AJT, Pellas P, Masarik J, Dreibus G (1996) Exposure history of the Torino meteorite. Meteoritics Planet Sci 31:265-272

Wieler R, Pedroni A, Leya I (2000a) Cosmogenic neon in mineral separates from Kapoeta: No evidence for an irradiation of its parent body regolith by an early active Sun. Meteoritics Planet Sci 35:251-257

Wieler R, Baur H, Jull AJT, Klandrud SE, Kring DA, Leya I, McHargue LR (2000b) Cosmogenic helium, neon, and argon in the large Gold Basin chondrite. Meteoritics Planet Sci 35:A169-A170

Wisdom J (1983) Chaotic behaviour and the origin of the 3/1 Kirkwood gap. Icarus 56:51-74

Woolum DS, Hohenberg C (1993) Energetic particle environment in the early solar system—extremely long pre-compaction meteoritic ages or an enhanced early particle flux. *In* Protostars and Planets III. Levy EH, Lunine JI (eds) Univ Arizona Press, Tucson, p 903-919

Wright RJ, Simms LA, Reynolds MA, Bogard DD (1973) Depth variation of cosmogenic noble gases in the ~120-kg Keyes chondrite. J Geophys Res 78:1308-1318

5 Cosmic-Ray-Produced Noble Gases in Meteorites

Rainer Wieler